Wnt/IL-1β/IL-8 autocrine circuitries control chemoresistance in mesothelioma initiating cells by inducing ABCB5

Wnt/IL-1β/IL-8 autocrine circuitries control chemoresistance in mesothelioma initiating cells by inducing ABCB5

Vladan Milosevic[1], Joanna Kopecka[1], Iris C Salaroglio[1], Roberta Libener[2], Francesca Napoli[1 3], Stefania Izzo[1 3], Sara Orecchia[2], Preeta Ananthanarayanan[1], Paolo Bironzo[1 4], Federica Grosso[5], Fabrizio Tabbò[1 4], Valentina Comunanza[1 6], Teodora Alexa-Stratulat[1], Federico Bussolino[1 6], Luisella Righi[1 3], Silvia Novello[1 4], Giorgio V Scagliotti[1 4], Chiara Riganti[1 7]

Affiliations

1 Department of Oncology, University of Torino, Torino, Italy.

2 Pathology Division, S. Antonio and Biagio Hospital, Alessandria, Italy.

3 Pathology Unit, Department of Oncology at San Luigi Hospital, University of Torino, Orbassano, Italy.

4 Thoracic Oncology Unit and Medical Oncology Division, Department of Oncology at San Luigi Hospital, University of Torino, Orbassano, Italy.

5 Oncology Division, S. Antonio and Biagio Hospital, Alessandria, Italy.

6 Candiolo Cancer Institute - FPO IRCCS, Candiolo, Italy.

7 Interdepartmental Center "G. Scansetti" for the Study of Asbestos and Other Toxic Particulates, University of Torino, Torino, Italy.

Abstract

Malignant pleural mesothelioma (MPM) is a tumor with high chemoresistance and poor prognosis. MPM-initiating cells (ICs) are known to be drug resistant, but it is unknown if and how stemness-related pathways determine chemoresistance. Moreover, there are no predictive markers of IC-associated chemoresistance. Aim of this work is to clarify if and by which mechanisms the chemoresistant phenotype of MPM IC was due to specific stemness-related pathways. We generated MPM IC from primary MPM samples and compared the gene expression and chemo-sensitivity profile of IC and differentiated/adherent cells (AC) of the same patient. Compared to AC, IC had upregulated the drug efflux transporter ABCB5 that determined resistance to cisplatin and pemetrexed. ABCB5-knocked-out (KO) IC clones were resensitized to the drugs in vitro and in patient-derived xenografts. ABCB5 was transcriptionally activated by the Wnt/GSK3β/β-catenin/c-myc axis that also increased IL-8 and IL-1β production. IL-8 and IL-1β-KO IC clones reduced the c-myc-driven transcription of ABCB5 and reacquired chemosensitivity. ABCB5-KO clones had lower IL-8 and IL-1β secretion, and c-myc transcriptional activity, suggesting that either Wnt/GSK3β/β-catenin and IL-8/IL-1β signaling drive c-myc-mediated transcription of ABCB5. ABCB5 correlated with lower time-to-progression and overall survival in MPM patients treated with cisplatin and pemetrexed. Our work identified multiple autocrine loops linking stemness pathways and resistance to cisplatin and pemetrexed in MPM IC. ABCB5 may represent a new target to chemosensitize MPM IC and a potential biomarker to predict the response to the first-line chemotherapy in MPM patients.

Abbreviations

ABC	ATP-binding cassette
AC	adherent cells
ALDH	aldehyde dehydrogenase
ANOVA	analysis of variance
ChIP	chromatin immunoprecipitation
CSF1R	colony-stimulating-factor-1-receptor
DAPI	4’,6-diamidino-2-phenylindole dihydrochloride
FBS	fetal bovine serum
FFPE	formalin-fixed paraffin-embedded
GFP	green fluorescence protein
GSK3β	glycogen synthase kinase 3β
i.p.	intraperitoneally
IC	initiating cells
KO	knocked-out
LDH	lactate dehydrogenase
LRP6	Low-density lipoprotein receptor-related protein 6
MPM	malignant pleural mesothelioma
myc-i	5-[(4-ethylphenyl)methylene]-2-thioxo-4-thiazolidinone
OS	overall survival
PFA	paraformaldehyde
PS	penicillin–streptomycin
RLU	relative luminescence units
s.c.	subcutaneously
SASP	senescence-associated secretory phenotype
SHH	Sonic Hedgehog
SOX	sex-determining region Y-box 2
TBP	TATA-Box Binding Protein
TBS	Tris-buffered saline
TTP	time to progression
UPN	unknown patient number

Introduction

Malignant pleural mesothelioma (MPM) is an asbestos-related tumor characterized by three histotypes, that is, epithelioid, biphasic and sarcomatous, mostly diagnosed in advanced stage and with an overall dismal prognosis. Platinum-based (cisplatin/carboplatin) chemotherapy in combination with antifolate agents (pemetrexed, raltitrexed) is a standard of care for advanced stage disease.1 Immunotherapy, targeted therapies2 and tumor microenvironment-targeting approaches3 are still under development. All treatments produce only partial responses, because of the strong chemoresistance of MPM.1

Tumor-initiating cells (IC) or cancer stem cells represent a small subpopulation of tumor bulk, but they are the main responsible for tumor mass renewal, recurrence and chemoresistance.4

MPM IC were first identified from commercial cell lines as a side population, ranging from 0.05 to 1.32% cells, positive for CD133, CD9, CD24, CD26, CD44, octamer-binding transcription factor 4 (Oct4), Nanog, sex-determining region Y-box 2 (SOX2), ATP-binding cassette transporter G2 (ABCG2), aldehyde dehydrogenase (ALDH).5-11 A shared feature of IC is their resistance to cisplatin and pemetrexed.6-9, 11, 12 The CD24- and CD26-downstream signaling,13 the senescence-associated secretory phenotype (SASP) kinase/STAT3 axis7 and the colony-stimulating-factor-1-receptor (CSF1R)/Akt/β-catenin axis8 contribute to the resistance to pemetrexed.

Until now, there are neither reports linking classical stemness pathways, such as Wnt-, Notch-, Sonic Hedgehog (SHH)-dependent pathways and chemoresistance, nor investigating the clinical implications of these linkages.

In different tumors, the chemoresistance of IC have been related to the overexpression of multiple ABC transporters that efflux a broad spectrum of chemotherapeutic and targeted-therapy agents.4 ABCG2 has been detected in MPM IC,14 where its expression has been correlated with resistance to cisplatin and pemetrexed.6, 15 Recently, ABCB5 was identified as a transporter mediating resistance to 5-fluorouracil in colon cancer side-population cells,16 and resistance to taxanes, Vinca alkaloids, doxorubicin, etoposide, teniposide and dacarbazine in melanoma ICs.17 No data on ABCB5 expression and role in the highly chemoresistant phenotype of MPM exist.

The aim of the present work is to investigate whether ABCB5 determines chemoresistance in MPM IC and whether specific stemness pathways activated in MPM IC are implicated in ABCB5-mediated chemoresistance. By analyzing primary cells of MPM patients, we aim at identifying new biomarkers predictive of poor response to the first-line chemotherapy, and possible druggable targets to induce chemosensitization.

Materials and Methods

Chemicals

Fetal bovine serum (FBS) and penicillin–streptomycin (PS) were supplied by Sigma Chemical Co. (St. Louis, MO), HAM F12 and DMEM medium were from Life Technologies (Milano, Italy), plastic ware for cell culture was from Falcon (BD Biosciences, Bedford, MA). Electrophoresis reagents were from Bio-Rad Laboratories (Hercules, CA). The protein content of cell monolayers and cell lysates was assessed with the bicinchoninic acid kit (Sigma Chemical Co.). Cisplatin and pemetrexed as the other reagents, if not otherwise specified, were purchased from Sigma Chemical Co.

Cells

Primary human MPM samples (3 epithelioid MPM, 1 sarcomatous MPM and 2 biphasic MPM) were obtained from diagnostic thoracoscopies, from the Biological Bank of Mesothelioma, S. Antonio e Biagio Hospital, Alessandria, Italy. Representative histologies of each MPM analyzed are reported in Supporting Information Figure S1. Patients were chemonaïve at the time of the thoracoscopies. Tissue was digested in medium containing 1 mg/ml collagenase and 0.2 mg/ml hyaluronidase for 1 hr at 37°C. The cell suspension was divided into two aliquots, to obtain differentiated/adherent cells (AC) and IC. To obtain AC, cells were cultured in HAM F12 medium supplemented with 10% FBS, 1% PS (AC medium). ICs were generated by maintaining cells in HAM F12/DMEM medium supplemented with 1% PS, 20 ng/ml of EGF, 20 ng/ml of β-FGF, 4 µg/ml of IGF, 0.2% v/v B27 (Invitrogen, Carlsbad, CA; IC medium). In these culture conditions, the first spheres with ≥50 cells were detectable after 2 weeks. From these cultures, we isolated Oct4+/Nanog+/SOX2+ cells by labeling cells with anti-Oct4/POU5F1 (rabbit #2750; Cell Signaling Technologies, Danvers, MA), anti-Nanog (rabbit mAb #4903; Cell Signaling Technologies) and anti-SOX2 (rabbit, #poly6308; BioLegend, San Diego, CA) antibodies, and sorting positive cells using a Cell Sorter BD FACSAria III (Becton Dickinson, Bedford, MA). The sorted population was let to grow for additional 2 weeks in IC medium; subsequently, ABCG2+/ALDHbright cells were sorted, after staining cells with an anti-ABCG2 antibody (mouse clone 5D3; Santa Cruz Biotechnology Inc., Santa Cruz, CA) and with the ALDEFLUOR™ kit (StemCell Technologies, Vancouver, Canada). These double-sorted cells were used for all the experiments reported. Either during subculture procedures or before preparing the samples for the experimental assays, spheres were dissociated in single cell suspension by repeated manual pipetting of the spheres floating in their culture medium. All patients were identified with unknown patient numbers (UPN). The Ethical Committee of Biological Bank of Mesothelioma approved the study (#9/11/2011). The mesothelial origin of the isolated cells was confirmed by positive immune-staining, as detailed previously.18 Cells were

authenticated by the STR analysis method and used until passage 6. Mycoplasma spp. contamination was checked by RT-PCR weekly; contaminated cells were discharged.

Stemness functional assays

Self-renewal and clonogenicity assays were performed as reported.19 For in vivo tumorigenicity assay, 1×10^8 AC or IC (3 mice/each UPN AC or IC), mixed with 100 µl Matrigel, were injected subcutaneously (s.c.) in 6-week-old female NOD-SCID-γ Balb/C mice (Charles River Laboratories Italia, Calco), housed (5 per cage) under 12 hr light/dark cycle, with food and drinking provided ad libitum. Tumor growth was measured daily by caliper, according to the equation $(L \times W^2)/2$, where L = tumor length and W = tumor width, up to 30 weeks.

qRT-PCR and high-throughput PCR arrays

Total RNA was extracted and reverse-transcribed using the iScript™ cDNA Synthesis Kit (Bio-Rad Laboratories). qRT-PCR was performed using IQ™ SYBR Green Supermix (Bio-Rad Laboratories). The primer sequences, designed with qPrimerDepot software (http://primerdepot.nci.nih.gov/), were: ABCB5: 5′-ATTGGAGTGGTTAGTCAAGAGCC-3′, 5′-AGTCACATCATCTCGTCCATACT-3′; IL-1β: 5′-ATGATGGCTTATTACAGTGGCAA-3′, 5′-GTCGGAGATTCGTAGCTGGA-3′; IL-8: 5′-ACTGAGAGTGATTGAGAGTGGAC-3′, 5′-AACCCTCTGCACCCAGTTTTC-3′; actin: 5′-GCTATCCAGGCTGTGCTATC-3′; 5′-TGTCACGCACGATTTCC-3′. PCR arrays were carried out on 1 µg cDNA, using Human Cancer Stem Cells RT^2 Profiler PCR Array, WNT Signaling Pathway RT^2 Profiler PCR Array, WNT Signaling Targets RT^2 Profiler PCR Array (Bio-Rad Laboratories) as per manufacturer's instructions. Data analysis was performed using the PrimePCR™ Analysis Software (Bio-Rad Laboratories).

Cytotoxicity and viability assays

The release of lactate dehydrogenase (LDH) in the extracellular medium, used as a sensitive index of drug cytotoxicity after 24 hr exposure,19 was measured by spectrophotometry, using a Synergy HT Multi-Detection Microplate Reader (BioTek Instruments, Winooski, VT). The results were expressed as percentage of extracellular LDH vs. total (intracellular plus extracellular) LDH. Viability was measured in cells incubated 72 hr, with the ATPlite Luminescence Assay System (PerkinElmer, Waltham, MA), as per manufacturer's instructions, using a Synergy HT Multi-Detection Microplate Reader. In preliminary dose–response experiments, AC and IC were incubated 72 hr with increasing concentrations (1 nM, 10 nM, 100 nM, 1 µM, 5 µM, 10 µM, 25 µM, 50 µM, 100 µM, 250 µM and 500 µM) of cisplatin and pemetrexed. The relative

luminescence units (RLU) of untreated cells were considered as 100% viability; results were expressed as a percentage of viable cells vs. untreated cells. IC_{50} and IC_{75} were defined as the concentrations of each drug that reduced cells viability to 50% and 25% compared to untreated cells, producing 50% and 75% cell death, respectively (GraphPad Prism, version 5).

Flow cytometry analysis

1×10^6 cells were rinsed and fixed with 2% w/v paraformaldehyde (PFA) for 2 min, permeabilized using 0.1% v/v Triton-X100 for 2 min on ice, washed three times with PBS and stained with the following antibodies: anti-Oct4, anti-Nanog; anti-SOX2; anti-ABCG2; anti-ABCB5 (rabbit SAB1300315; Sigma Chemical Co.); anti-Frizzled 1 (mouse clone E-7; Santa Cruz Biotechnology Inc.); anti-Frizzled 2 (rabbit ab219101; Abcam, Cambridge, UK); anti-Frizzled 3 (mouse clone C-1; Santa Cruz Biotechnology Inc.); antilow-density lipoprotein receptor-Related Protein 6 (LRP6, rabbit EPR2423 (2); Abcam) for 1 hr on ice, followed by an AlexaFluor 488-conjugated secondary antibody (Millipore, Billerica, MA) for 30 min. 1×10^5 cells were analyzed with EasyCyte Guava™ flow cytometer (Millipore), equipped with the InCyte software (Millipore). Control experiments included incubation with nonimmune isotype antibody.

Immunofluorescence analysis

5×10^5 AC were seeded onto glass coverslips in six-well plates overnight. IC were collect by cytospinning. All cells were fixed using 4% PFA w/v for 15 min, washed with PBS, permeabilized with 1% v/v Triton X-100 for 5 min, washed with PBS and incubated for 24 hr with anti-ABCB5 antibody (Sigma Chemicals Co.) or anti c-myc antibody (clone 9E10.3; Millipore), diluted 1:100 in 1% v/v FBS/PBS at 4°C. Samples were washed five times with PBS and incubated for 1 hr with fluorescein isothiocyanate- or tetramethylrhodamine isothiocyanate-conjugated secondary antibodies (Sigma Chemicals Co.), diluted 1:50. After this step, cells were incubated with 4',6-diamidino-2-phenylindole dihydrochloride (DAPI), diluted 1:1000 in PBS for 5 min, washed four times with PBS and once with deionized water. The coverslips were mounted with Gel Mount Aqueous Mounting and examined with a Leica DC100 fluorescence microscope (Leica Microsystems GmbH, Wetzlar, Germany). For each experimental point, a minimum of five microscopic fields were examined.

Generation of knocked-out clones

AC or IC were knocked-out (KO) for ABCB5, IL-1β or IL-8 using respective CRISPR/Cas9-green fluorescence protein (GFP)-plasmids (KN415604, KN402079, KN202075; Origene, Rockville, MD). Nontargeting (scrambled) CRISPR/Cas9 plasmid was used as control of specificity. Cells were seeded at 1×10^5 cells/ml in

PS-free medium. One microgram of CRISPR/Cas9 KO plasmid was used as per manufacturer's instructions. Transfected cells were sorted by isolating GFP-positive cells. Knocking-out efficacy was verified by qRT-PCR or immunoblotting. Stable KO-clones were generated by culturing cells for 6 weeks in medium containing 1 µg/ml puromycin.

***In vivo* chemosensitivity assay**

1×10^7 IC, stably transfected with a nontargeting (scrambled) CRISPR/Cas9 vector or with ABCB5-knock-out (KO) CRISPR/Cas9 vector, were inoculated s.c. in 9 weeks old NOD-SCID-γ Balb/C female mice. Tumor volume was monitored by caliper and calculated according to the equation: equation $(L \times W^2)/2$, where L = tumor length and W = tumor width. When tumors reached the volume of 50 mm^3, animals were randomized in the following groups (n = 6/for each group) and treated as it follows at day 1, 7, 14, 21, 28 and 35 after randomization: (i) scrambled vehicle, that is, animals bearing a scrambled-IC tumor receiving 200 µl solution saline intraperitoneally (i.p.); (ii) scrambled cisplatin plus pemetrexed, that is, animals bearing a scrambled-IC tumor, receiving 5 mg/kg cisplatin i.p. and 100 mg/kg pemetrexed i.p.; (iii) KO vehicle, that is, animals bearing a ABCB5 KO-IC tumor receiving 200 µl solution saline i.p.; (iv) KO cisplatin plus pemetrexed, that is, animals bearing a ABCB5 KO-IC tumor, receiving 5 mg/kg cisplatin i.p. and 100 mg/kg pemetrexed i.p. In preliminary experiments, we adopted 5 mg/kg cisplatin and 200 mg/kg pemetrexed, already used in 9 weeks old NOD-SCID-γ Balb/C female mice bearing patient-derived MPM:20 this dosage had the same efficacy of 5 mg/kg cisplatin and 100 mg/kg pemetrexed (data not shown), but induced a 20% mortality in the chemotherapy-treated mice between day 35 and 48. We chose the treatment with 5 mg/kg cisplatin and 100 mg/kg pemetrexed because it allowed a 100% survival until the euthanasia. Tumor volumes were monitored daily by caliper and animals were euthanized at day 48 after randomization with zolazepam (0.2 ml/kg) and xylazine (16 mg/kg). The hemocromocytometric analyses were performed with a UniCel DxH 800 Coulter Cellular Analysis System (Beckman Coulter, Miami, FL) on blood collected immediately after sacrificing the mice. Hematochemical parameters were analyzed using the respective kits from Beckman Coulter Inc. Animal care and experimental procedures were approved by the Bio-Ethical Committee of the Italian Ministry of Health (#122/2015-PR).

Immunoblotting

Cells were rinsed with ice-cold lysis buffer (50 mM Tris, 10 mM EDTA, 1% v/v Triton-X100; pH 7.5), supplemented with the protease inhibitor cocktail set III (Calbiochem. La Jolla, CA), 2 mM phenylmethylsulfonyl fluoride, 1 mM Na_3VO_4. Cells were then sonicated (10 bursts of 10 sec, 4°C, 100 W; Labsonic sonicator, Hielscher, Teltow, Germany) and centrifuged at 13,000 × g for 10 min at 4°C. About

20 µg protein extracts were subjected to 4–20% gradient SDS-PAGE and probed with the following antibodies, all diluted 1:1000 in Tris-buffered saline (TBS)-Tween nonfat dry milk 5%: antiglycogen synthase kinase 3β (GSK3β, rabbit mAb#9315; Cell Signaling Technologies), antiphospho(Tyr279/Tyr216)GSK3β (mouse, clone 5G-2F; Millipore), anti-β-catenin (rabbit mAb#8480, Cell Signaling Technologies), antiphospho(Ser33/37/Thr41)-β-catenin (rabbit #9561; Cell Signaling Technologies), anti-β-tubulin antibody (mouse clone D-10; Santa Cruz Biotechnology). Blotting was followed by the peroxidase-conjugated secondary antibody (Bio-Rad). The membranes were washed with TBS/Tween 0.01% v/v and proteins were detected by enhanced chemiluminescence (Bio-Rad Laboratories). To detect ubiquitinated β-catenin, 100 µg protein extracts were immunoprecipitated overnight with the anti-β-catenin antibody, using 25 µl of PureProteome Magnetic Beads (Millipore). Immunoprecipitated samples were then probed with an antimono/polyubiquitin antibody (mouse clone FK-2; Axxora, Lausanne, Switzerland). Blot images were acquired with a ChemiDoc™ Touch Imaging System device (Bio-Rad Laboratories). Nuclear extraction was performed using the Nuclear Extraction Kit (Active Motif, Rixensart, Belgium). 10 µg of nuclear proteins were subjected to immunoblotting and analyzed for β-catenin or TATA Box Binding Protein (TBP, mouse clone 1TB18; Santa Cruz Biotechnology Inc.) expression.

Chromatin immunoprecipitation

Chromatin immunoprecipitation (ChIP) samples were prepared as previously reported21 using a ChIP-tested anti-c-myc antibody (mouse clone 9E11; Abcam, Cambridge, UK). The putative c-Myc binding site on ABCB5 promoter was validated with the Matinspector software (https://www.genomatix.de/matinspector.html). Primer sequences were: 5'-CACAACTTCAAGTGGTAGCATG-3'; 5'-CCATTCTACCCAGTGAAATG-3'. Primers used as negative internal controls for a nonspecific 10,000 bp upstream sequence were: 5'-GTGGTGCCTGAGGAAGAGAG-3'; 5'-GCAACAAGTAGGCACAAGCA-3'. The immunoprecipitated products were amplified by qRT-PCR.

GSK3β, RhoA and RhoA kinase activity

The kinase activity of GSK3β was measured on the protein immunopurified from cell extracts by a radiometric assay, using the GSK-3β Activity Assay Kit (Sigma Chemicals. Co), as per manufacturer's instructions. Results were expressed as count per minute (cpm)/mg cellular proteins. Rho-GTP considered an index of active RhoA, and RhoA kinase activity, were measured by spectrophotometric methods, using the G-LISA RhoA Activation Assay Biochem Kit (Cytoskeleton, Denver, CO) and the CycLex Rho Kinase Assay Kit (CycLex, Nagano, Japan), respectively. Results were expressed as U absorbance/mg cell proteins,

according to titration curves prepared with serial dilutions of Rho-GTP positive control (Cytoskeleton) and recombinant RhoA kinase (MBL, Woburn, MA).

Cytokine production

IL-1β and IL-8 levels were measured in the culture supernatants using the human IL-8(CXCL8) TMB ELISA Development Kit (PeproTech, London, UK) and the human IL-1β/IL-1F2 ELISA kit (DuoSet ELISA, R&D Systems, Minneapolis, MN), as per manufacturer's instructions.

Immunohistochemistry

Formalin-fixed paraffin-embedded (FFPE) samples of chemonaïve patients with confirmed histological diagnosis of MPM were retrospectively analyzed for the expression of ABCB5 (rabbit ab203120; Abcam). All patients were then treated with cisplatin/carboplatin plus pemetrexed as first-line therapy. ABCB5 was considered positive when a weak-to-strong membrane or cytosolic positivity was shown. The tumor proportion positivity was recorded. Patients were divided into $ABCB5^{low}$ and $ABCB5^{high}$, if the tumor proportion of ABCB5 staining was respectively below or equal/above the median value.

Statistical analysis

All data in the text and figures are provided as means ± SD. The results were analyzed by a one-way analysis of variance (ANOVA), using Statistical Package for Social Science (SPSS) software (IBM SPSS Statistics version 19). A value of $p < 0.05$ was considered significant. The Kaplan–Meier method was used to calculate the time to progression (TTP: time from the start of treatment to the first sign of disease's progression) and overall survival (OS: survival from the beginning of chemotherapy until patients' death). Log-rank test was used to compare the outcome of $ABCB5^{low}$ and $ABCB5^{high}$ groups. The sample size was calculated with the G*Power software (www.gpower.hhu.de), setting $\alpha \leq 0.05$ and $1 - \beta = 0.80$. Researchers analyzing the results were unaware of the treatments received.

Results

Phenotypic and functional characterization of MPM ICs

Six MPM samples, representative of the three main histotypes (i.e., epithelioid, sarcomatous and biphasic), were obtained from patients with annotated clinical data (Supporting Information Table S1) and histopathological characterization (Supporting Information Table S2). From each patient, AC and IC were obtained (Fig. 1a), as detailed under Materials and methods. IC had strong positivity for the general stemness markers ALDH, Oct4, Nanog, SOX2 and ABCG2 (Figs. 1b and 1c). For all the histotypes, IC showed significantly higher self-renewal (Fig. 1d), in vitro clonogenicity (Fig. 1e) and in vivo tumorigenicity (Supporting Information Table S3) compared to AC, displaying the key phenotypic and functional properties of IC.

Targeted-gene expression analysis confirmed that general stemness markers were upregulated, developmental and differentiation markers were either upregulated or downregulated. Notch-related genes were mostly downregulated, while genes associated with Wnt and SHH pathways were mostly upregulated. No clear signatures of increased proliferation, survival, epithelial–mesenchimal transition, adhesion and migration differentiated IC from AC (Fig. 1e; Supporting Information Table S1).

ABCB5 determines chemoresistance in MPM IC

AC and IC were cultured for 72 hr in the presence of increasing concentrations (ranging from 1 nM to 500 μM) of cisplatin and pemetrexed, then the cell viability was measured. The dose–response viability curves of each patient indicated a higher IC50 in all IC compared to AC (Supporting Information Fig. S2). About 25 μM cisplatin and 5 μM pemetrexed were chosen because they were between the IC50 and the IC75 for all AC. At these concentrations, IC did not show any acute cell damage, measured as increase of extracellular LDH after 24 hr (Fig. 2a), nor any reduction in cell viability after 72 hr (Fig. 2b), differently from AC.

Since ABCB5, a transporter of several drugs present in tumor IC,16, 17, 22 was significantly upregulated in six out of six IC compared to AC (Fig. 1e), we investigated its role in MPM IC chemoresistance. ABCB5 was significantly upregulated in all the histotypes of MPM IC as mRNA (Fig. 2c) and protein, either in cytosol (Fig. 2d), that is, the newly synthesized protein moving from endoplasmic reticulum to plasma-membrane, or on cell surface (Fig. 2e), that is, the active protein form. ABCB5-KO IC (Fig. 2f) markedly rescued the sensitivity to cisplatin and pemetrexed, in terms of increased cell damage (Fig. 2g) and reduced viability (Fig. 2h). IC-patient derived xenografts of epithelioid and sarcomatous MPM were resistant to the combination of cisplatin and pemetrexed. In contrast, chemotherapy significantly reduced tumor growth

and tumor volume (Figs. 2i and 2j) of IC-derived ABCB5-KO tumors derived from the same patient. None of the treatment group had signs of systemic toxicity according to the hematochemical parameters (Supporting Information Table S5). Overall, these data indicate that ABCB5 contributes to the chemoresistance in MPM IC.

ABCB5 is necessary to induce stemness properties in MPM cells

To investigate if ABCB5 plays a role in the acquisition or maintenance of a stemness phenotype, we stably KO ABCB5 from UPN1 and UPN4 AC. After the selection in AC medium containing puromycin, the stably KO clones, were cultured for 2 weeks in IC medium, generating the so-called KO-ABCB5-AC. These cells were compared to AC and IC (indicated as wt-AC and wt-IC in Fig. 3), generated as reported in the Materials and Methods section (Fig. 3a). KO-ABCB5-AC had undetectable levels of ABCB5, similar to wt-AC and lower than wt-IC generated from the same patient (Fig. 3b). Differently, from wt-AC (reported in Fig. 1a, upper panels), KO-ABCB5-AC grew as spheres when cultured in IC medium, but they formed smaller spheres than wt-IC (Fig. 3c). The levels of classical stemness markers Oct4, Nanog, SOX2 and ABCG2 were lower in KO-ABCB5-AC than in wt-IC and comparable to the levels of wt-AC of the same patient (Fig. 3d). Moreover, KO-ABCB5-AC had very low self-renewal and clonogenic potential, behaving like wt-AC (Figs. 3e and 3f).

In contrast, the knock-out of ABCB5 in already established IC, producing the KO-ABCB5-IC clones, did not reduce spheres volume, percentage of $Oct4^+$, $Nanog^+$, $SOX2^+$ and $ABCG2^+$ cells, self-renewal and clonogenicity potential (Figs. 3b–3f).

The canonical Wnt/GSK3β/β-catenin pathway is upregulated in MPM IC

Previous findings demonstrate that Wnt pathway induces chemoresistance by upregulating ABC transporters,19, 23-25 but the upregulation of ABCB5 has not been yet investigated. Since some Wnt-related genes were upregulated in MPM IC (Fig. 1e), we focused on their possible involvement in the chemoresistance mediated by ABCB5. Notable, most Wnt ligands, Wnt-receptors belonging to Frizzled family, activating Wnt-transducers of canonical pathway were significantly upregulated in IC, whereas most soluble Wnt inhibitors and negative transducers were downregulated (Fig. 4a; Supporting Information Table S6). In keeping with this signature, Frizzled 1, Frizzled 2 and Frizzled 3 receptors, but not the coreceptor LRP6, were higher in IC (Fig. 4b). Phospho(Tyr279/Tyr216)GSK3β, that is, the active GSK3β, and phospho(Ser33/Ser37/Thr41)-β-catenin, that is, the protein-primed for ubiquitination and proteasomal degradation, were undetectable in IC (Fig. 4c). Consistently, ubiquitinated β-catenin was lower in IC (Fig. 4d), indicating an increased activity of the Wnt/GSK3β/β-catenin axis. Cytosolic β-catenin, indicating the amount of protein not ubiquitinated, was higher in IC than in AC (Fig. 4e, left panel). Nuclear β-catenin IC,

corresponding to the transcriptionally activated form, was higher in IC as well (Fig. 4e, right panel). Consistently, several target genes of Wnt canonical pathway resulted upregulated in IC, as demonstrated by global gene expression profile (Fig. 4a; Supporting Information Table S6).

The GSK3β/β-catenin/c-myc axis upregulates ABCB5 in MPM ICs

c-myc is a target gene of Wnt/GSK3β/β-catenin axis26 and a transcriptional factor for ABCB5.27 To test if it may represent the possible link between Wnt pathway and ABCB5 in MPM, we treated IC with 250 μM of c-myc inhibitor 5-[(4-ethylphenyl)methylene]-2-thioxo-4-thiazolidinone (myc-i), a concentration that fully abrogated c-myc transcriptional activity on ABCB5 (Supporting Information Fig. S3), consistently with previous dose-dependence experiments.27 Using a complementary approach, we treated AC with 10 mM of the GSK3β inhibitor LiCl that inhibited the phosphorylation activity of GSK3β (Supporting Information Fig. S4) and activates Wnt canonical pathway in glioblastoma-derived cancer stem cells.20 In LiCl-treated AC, c-myc was more translocated into the nucleus (Fig. 5a) and more bound to ABCB5 promoter (Fig. 5b). Consistently, the transcription of ABCB5 was increased (Fig. 5c) and the cytotoxicity exerted by cisplatin and pemetrexed was reduced (Fig. 5d). In contrast, myc-i prevented the nuclear translocation of c-myc in IC (Fig. 5a), reduced c-myc binding on ABCB5 promoter (Fig. 5b) and ABCB5 mRNA levels (Fig. 5c), resensitized IC to the cytotoxic effects of cisplatin and pemetrexed (Fig. 5d). These data provide the proof of concept that ABCB5 is under the control of GSK3β/β-catenin/c-myc axis and that the inhibition of this pathway chemosensitizes MPM IC.

Although the gene of RhoA, a noncanonical Wnt-transducer, was upregulated in MPM IC (Fig. 4a) and RhoA was more active in IC than in AC (Supporting Information Fig. S5a), the RhoA/RhoA kinase axis was not involved in the upregulation of ABCB5: indeed, when RhoA kinase was inhibited by Y27632 (Supporting Information Fig. S5b), neither c-myc binding to ABCB5 promoter (Supporting Information Fig. S5c) nor ABCB5 mRNA (Supporting Information Fig. S5d) were modified compare to untreated MPM IC.

Wnt-driven autocrine production of IL-8 and IL-1β contributes to upregulate ABCB5 in MPM IC

In melanoma-IC, ABCB5 secretes IL-1β that stimulates ABCB5-negative cells to increase the production of IL-8: IL-8 in turn upregulates ABCB5 in tumor IC.17 To explore whether an IL-1β/IL-8 loop is active also in MPM, we first screened the expression of cytokine genes in MPM cultures. Among the 84 cytokines mRNAs detectable in MPM cells, IL-8 and IL-1β were the highest cytokines expressed in IC compared to AC (Fig. 6a). The higher mRNA levels (Figs. 6b and 6c) were paralleled by the higher amount of both cytokines in the culture medium (Figs. 6d and 6e) of IC (termed IC scr in Fig. 6). The production of IL-8 and IL-1β was controlled by Wnt/GSK3β/β-catenin/c-myc axis: indeed, AC treated with LiCl increased the production of IL-

8 and IL-1β, while IC treated with myc-i reduced the amount of both cytokines (Figs. 6f and 6g). Our results are consistent with previous findings reporting that IL-8 and IL-1β are targets of β-catenin28, 29 and c-myc.30, 31 Interestingly, IL-8-KO and IL-1β-KO IC clones, characterized by nearly undetectable levels of cytokines mRNA (Figs. 6b and 6c) and protein (Figs. 6d and 6e), had lower binding of c-myc to ABCB5 promoter (Fig. 6h) and lower ABCB5 mRNA (Fig. 6i). Accordingly, IL-8 and IL-1β-KO IC clones were significantly more sensitive to cisplatin and pemetrexed cytotoxicity (Fig. 6j).

ABCB5-KO clones (Supporting Information Fig. S6a) had a lower secretion of IL-8 and IL-1β (Supporting Information Fig. S6b and S6c). Of note, ABCB5-KO IC had a lower binding of c-myc to the promoter of ABCB5 compared to parental (scr) IC: the binding was increased by exogenous IL-8 and IL-1β (Supporting Information Fig. S6d), added at a concentration that restored IL-8 and IL-1β to levels comparable to parental IC (Supporting Information Fig. S6e and S6f).

These results highlighted that ABCB5 induces chemoresistance in IC, where it is upregulated by multiple autocrine circuitries (Fig. 5k).

ABCB5 is predictive of poor response to chemotherapy in patients with MPM

In the FFPE, MPM samples of 37 patients (34 epithelioid, 2 sarcomatous, 1 biphasic MPM), treated with cisplatin plus pemetrexed (Supporting Information Table S7), ABCB5 was detected—before chemotherapeutic treatment—in isolated cells or clusters (Fig. 7a), in particular in plasma-membrane (Fig. 7b). The median staining intensity of ABCB5 in MPM cells (Supporting Information Table S7) was used to dichotomize patients in $ABCB5^{low}$ and $ABCB5^{high}$ groups. As shown in Figures 7c and 7d, $ABCB5^{high}$ group had significantly lower TTP and OS, suggesting that ABCB5 expression is predictive of poorer response to the first-line chemotherapy and poorer outcome in MPM patients.

Discussion

In this work, we isolated and characterized MPM IC from patient biopsies and we demonstrated that they are resistant to cisplatin and pemetrexed. We suggest that the presence of IC within MPM bulk contributes to the high chemoresistance of this tumor in patients. We identified ABCB5 as a crucial efflux transporter mediating resistance to cisplatin and pemetrexed in MPM IC. Besides its role in chemoresistance, ABCB5 can be considered an essential factor in the acquisition of stemness properties. Indeed, KO-ABCB5-AC clones formed smaller spheres than IC and did not show phenotypic markers and functional properties of stemness, notwithstanding their growth in IC medium that favors the expansion of IC-enriched populations. We hypothesize that ABCB5 loss attenuates the stemness potential in the MPM cell population, while knocking-out ABCB5 in established IC did not promote cell differentiation, as demonstrated by KO-ABCB5-IC clones that are phenotypically and functionally identical to parental IC. Once the stem cell-like phenotype is generated, ABCB5 is not necessary to maintain stemness, but it is crucial to determine chemoresistance, under the control of the highly conserved, stemness-related Wnt pathway.

Previous findings reported a constitutive activation of the Disheveled/GSK3β/β-catenin pathway in MPM32-34 in commercial cell lines or tumor bulk. We demonstrated that the canonical Wnt/GSK3β/β-catenin pathway was specifically activated in MPM IC, leading to the upregulation of several β-catenin-target genes involved in proliferation, invasion, angiogenesis and chemoresistance.

Wnt pathway inhibitors emerged as antiproliferative strategies and chemosensitizers in MPM.35-39 However, no studies investigated if the chemosensitization was due to the specific targeting of IC.

Our work indicated that ABCB5 induces constitutive resistance to cisplatin and pemetrexed in IC derived from MPM patients. We cannot exclude a priori that other ABC transporters expressed in MPM IC, such as ABCG2 and ABCB1, another target of Wnt pathway,19 mediate chemoresistance. Recently, we also found ABCB2, ABCC1, ABCC6 overexpressed in UPN1, UPN4 and UPN6-derived IC, compared to AC.40 Cisplatin is a substrate of ABCC1 and ABCC6; pemetrexed is poorly recognized by all these transporters.41, 42 In contrast, ABCB5 is known to induce resistance to carboplatin22 and to recognize a broad spectrum of chemotherapeutic drugs.17 Hence, it may determine a multidrug resistant phenotype in MPM IC.

We propose that interconnected mechanisms upregulate ABCB5 in MPM IC. First, Wnt/GSK3β/β-catenin/c-myc axis induced ABCB5 transcription, as demonstrated by the pharmacological inhibition of Wnt/GSK3β/β-catenin/c-myc axis. Second, IL-8/c-myc and IL-1β/c-myc axis upregulated ABCB5, as demonstrated by IL-8 and IL-1β-KO clones. Partially in disagreement with our data, Wilson and colleagues proposed that ABCB5 is upstream Wnt pathway in melanoma tumor IC, where ABCB5 and Wnt pathways are upregulated by IL-8 and IL-1β.17 In MPM IC, the pharmacological inhibition of Wnt/c-myc axis demonstrated that this axis controls the production of both IL-8 and IL-1β, suggesting that IL-8 and IL-1β are targets and controllers of

β-catenin/c-myc transcriptional program. Differently, from melanoma, that requires a paracrine cooperation between ABCB5-positive and ABCB5-negative cells to maintain high levels of IL-1β and IL-8, and chemoresistance,17 MPM IC adopted a completely autocrine system. Indeed, ABCB5-KO clones had lower secretion of IL-8 and IL-1β, suggesting that ABCB5 controls the secretion of both cytokines, and lower binding of c-myc to ABCB5 promoter, restored by exogenous IL-8 and IL-1β. These results support the hypothesis that Wnt/GSK3β/β-catenin/c-myc/ABCB5 axis, IL-8/c-myc/ABCB5 axis and IL-1β/c-myc/ABCB5 axis are part of feed-forward circuitries that maintain chemoresistance in MPM IC.

The clinical meaning of ABCB5 was validated in a retrospective series of chemonaïve MPM patients, who then received platinum-derivatives and pemetrexed. Of note, patients highly expressing ABCB5 had significantly lower TTP and OS. ABCB5 was positively associated with tumor progression and recurrence in oral squamous cell carcinomas,43 but, to the best of our knowledge, this is the first time that ABCB5 emerged as a potential marker of chemoresistance. The patients series analyzed was limited. Since ABCB5 can be easily detected by immunohistochemistry analysis, its expression is being evaluated in a larger cohort of MPM patients, to strengthen its predictive value.

Our study indicates that IC determines chemoresistance in MPM and provides the first evidence of a molecular link between the classical stemness-related Wnt pathway and the chemoresistance related to ABC transporters, namely, ABCB5. ABCB5 is a trigger of both stemness and chemoresistance in MPM. Its reduction, by targeting Wnt-pathway or IL-8/IL-1β signaling, chemosensitizes MPM IC. We also suggest to include the analysis of ABCB5 levels in the diagnostic assessment of MPM patients, as a potential stratification marker identifying patients more resistant to the first-line chemotherapy.

Acknowledgements

This work was supported by the Italian Association for Cancer Research (IG21408 to CR); Italian Ministry of University and Research (Future in Research program RBFR12SOQ1 to CR; Basic research Funding program, FABR2017 to LR and CR); Italian Ministry of Health (GR-2011-02348356 to LR; Italian Mesothelioma Network-CCM2012 to GVS); Azienda Ospedaliera "S. Antonio e Biagio e Cesare Arrigo" to GVS for the research activity "MESOLINE"; ERA-Net Transcan-2-JTC 2017 (TOPMESO to FB); University of Torino (Intramural Grant 2015 to SN and CR; Intramural Grant 2016 to LR; Intramural Grant 2017 to JK); Fondazione Cassa di Risparmio di Torino (2016-2443 to CR). VM is a PhD fellow of Erasmus Mundus-ERAWEB Action 2 program. ICS is a postdoctoral research fellow supported by the Fondazione Franco e Marilisa Caligara for Multidisciplinary Sciences, Torino, Italy. TA-S is a fellow of Trialect Inc., Global Medical Education Program. The funding institutions had no role in the study design, data collection and analysis, or in writing the article. We are grateful to Mr. Costanzo Costamagna, Department of Oncology, University of Torino, and to Dr. Erika Ortolan, Department of Medical Sciences, University of Torino, for the technical assistance.

References

1. Remon J, Reguart N, Corral J, et al. Malignant pleural mesothelioma: new hope in the horizon with novel therapeutic strategies. Cancer Treat Rev 2015; 41: 27–34.
2. McCambridge AJ, Napolitano A, Mansfield AS, et al. Progress in the Management of Malignant Pleural Mesothelioma in 2017. J Thorac Oncol 2018; 13: 606–23.
3. Fennell DA. Targeting the tumour vasculature in mesothelioma. Lancet Oncol 2018; 19: 723–4.
4. Zhao J. Cancer stem cells and chemoresistance: the smartest survives the raid. Pharmacol Ther 2016; 160: 145–58.
5. Kai K, D'Costa S, Yoon BI, et al. Characterization of side population cells in human malignant mesothelioma cell lines. Lung Cancer 2010; 70: 146–51.
6. Cortes-Dericks L, Carboni GL, Schmid RA, et al. Putative cancer stem cells in malignant pleural mesothelioma show resistance to cisplatin and pemetrexed. Int J Oncol 2010; 37: 437–44.
7. Canino C, Mori F, Cambria A, et al. SASP mediates chemoresistance and tumor-initiating-activity of mesothelioma cells. Oncogene 2012; 31: 3148–63.
8. Cioce M, Canino C, Goparaju C, et al. Autocrine CSF-1R signaling drives mesothelioma chemoresistance via AKT activation. Cell Death Dis 2014; 5:e1167.
9. Cortes-Dericks L, Froment L, Boesch R, et al. Cisplatin-resistant cells in malignant pleural mesothelioma cell lines show ALDH(high)CD44(+) phenotype and sphere-forming capacity. BMC Cancer 2014; 14:e304.
10. Pasdar EA, Smits M, Stapelberg M, et al. Characterisation of mesothelioma-initiating cells and their susceptibility to anti-cancer agents. PLoS One 2015; 10:e0119549.
11. Blum W, Pecze L, Felley-Bosco E, et al. Stem cell factor-based identification and functional properties of in vitro-selected subpopulations of malignant mesothelioma cells. Stem Cell Rep 2017; 8: 1005–17.
12. Wu L, Blum W, Zhu CQ, et al. Putative cancer stem cells may be the key target to inhibit cancer cell repopulation between the intervals of chemoradiation in murine mesothelioma. BMC Cancer 2018; 18:e471.
13. Yamazaki H, Naito M, Ghani FI, et al. Characterization of cancer stem cell properties of CD24 and CD26-positive human malignant mesothelioma cells. Biochem Biophys Res Commun 2012; 419: 529–36.
14. Fischer B, Frei C, Moura U, et al. Inhibition of phosphoinositide-3 kinase pathway down regulates ABCG2 function and sensitizes malignant pleural mesothelioma to chemotherapy. Lung Cancer 2012; 78: 23–9.
15. Frei C, Opitz I, Soltermann A, et al. Pleural mesothelioma side populations have a precursor phenotype. Carcinogenesis 2011; 32: 1324–32.

16. Wilson BJ, Schatton T, Zhan Q, et al. ABCB5 identifies a therapy-refractory tumor cell population in colorectal cancer patients. Cancer Res 2011; 71: 5307–16.
17. Wilson BJ, Saab KR, Ma J, et al. ABCB5 maintains melanoma-initiating cells through a proinflammatory cytokine signaling circuit. Cancer Res 2014; 74: 4196–207.
18. Kopecka J, Salaroglio IC, Righi L, et al. Loss of C/EBP-β LIP drives cisplatin resistance in malignant pleural mesothelioma. Lung Cancer 2018; 120: 34–45.
19. Riganti C, Salaroglio IC, Caldera V, et al. Temozolomide downregulates P-glycoprotein expression in glioblastoma stem cells by interfering with the Wnt3a/glycogen synthase-3 kinase/β-catenin pathway. Neuro Oncol 2013; 15: 1502–17.
20. Wu L, Allo G, John T, et al. Patient-derived xenograft establishment from human malignant pleural mesothelioma. Clin Cancer Res 2017; 23: 1060–7.
21. Campia I, Sala V, Kopecka J, et al. Digoxin and ouabain induce the efflux of cholesterol via liver X receptor signalling and the synthesis of ATP in cardiomyocytes. Biochem J 2012; 447: 301–11.
22. Kleffel S, Lee N, Lezcano C, et al. ABCB5-targeted chemoresistance reversal inhibits Merkel cell carcinoma growth. J Invest Dermatol 2016; 136: 838–46.
23. Su HY, Lai HC, Lin YW, et al. Epigenetic silencing of SFRP5 is related to malignant phenotype and chemoresistance of ovarian cancer through Wnt signaling pathway. Int J Cancer 2010; 127: 555–67.
24. Luo K, Gu X, Liu J, et al. Inhibition of disheveled-2 resensitizes cisplatin-resistant lung cancer cells through down-regulating Wnt/β-catenin signaling. Exp Cell Res 2016; 347: 105–13.
25. Cai J, Fang L, Huang Y, et al. Simultaneous overactivation of Wnt/β-catenin and TGFβ signalling by miR-128-3p confers chemoresistance-associated metastasis in NSCLC. Nat Commun 2017; 8:e15870.
26. Juan J, Muraguchi T, Iezza G, et al. Diminished WNT -> β-catenin -> c-MYC signaling is a barrier for malignant progression of BRAFV600E-induced lung tumors. Genes Dev 2014; 28: 561–75.
27. Kugimiya N, Nishimoto A, Hosoyama T, et al. The c-MYC-ABCB5 axis plays a pivotal role in 5-fluorouracil resistance in human colon cancer cells. J Cell Mol Med 2015; 19: 1569–81.
28. Lévy L, Neuveut C, Renard CA, et al. Transcriptional activation of interleukin-8 by beta-catenin-Tcf4. J Biol Chem 2002; 277: 42386–93.
29. Aumiller V, Balsara N, Wilhelm J, et al. WNT/β-catenin signaling induces IL-1β expression by alveolar epithelial cells in pulmonary fibrosis. Am J Respir Cell Mol Biol 2013; 49: 96–104.
30. Liu T, Zhou Y, Ko KS, et al. Interactions between Myc and mediators of inflammation in chronic liver diseases. Mediators Inflamm 2015; 2015:e276850.
31. Shchors K, Shchors E, Rostker F, et al. The Myc-dependent angiogenic switch in tumors is mediated by interleukin 1beta. Genes Dev 2006; 20: 2527–38.

32. Fox SA, Richards AK, Kusumah I, et al. Expression profile and function of Wnt signaling mechanisms in malignant mesothelioma cells. Biochem Biophys Res Commun 2013; 440: 82–7.
33. Uematsu K, Kanazawa S, You L, et al. Wnt pathway activation in mesothelioma: evidence of dishevelled overexpression and transcriptional activity of beta-catenin. Cancer Res 2003; 63: 4547–51.
34. Anani W, Bruggeman R, Zander DS. β-Catenin expression in benign and malignant pleural disorders. Int J Clin Exp Pathol 2011; 4: 742–7.
35. Sato A, Ueno H, Fusegi M, et al. Succinate ether derivative of tocotrienol enhances Dickkopf-1 gene expression through epigenetic alterations in malignant mesothelioma cells. Pharmacology 2018; 102: 26–36.
36. Barbarino M, Cesari D, Intruglio R, et al. Possible repurposing of pyrvinium pamoate for the treatment of mesothelioma: a pre-clinical assessment. J Cell Physiol 2018; 233: 7391–401.
37. Moriyama G, Tanigawa M, Sakai K, et al. Synergistic effect of targeting dishevelled-3 and the epidermal growth factor receptor-tyrosine kinase inhibitor on mesothelioma cells in vitro. Oncol Lett 2018; 15: 833–8.
38. Mazieres J, You L, He B, et al. Wnt2 as a new therapeutic target in malignant pleural mesothelioma. Int J Cancer 2005; 117: 326–32.
39. Uematsu K, Seki N, Seto T, et al. Targeting the Wnt signaling pathway with dishevelled and cisplatin synergistically suppresses mesothelioma cell growth. Anticancer Res 2007; 27: 4239–42.
40. Riganti C, Contino M, Guglielmo S, et al. Design, biological evaluation and molecular modelling of tetrahydroisoquinoline derivatives: discovery of a potent P-glycoprotein ligand overcoming multi-drug resistance in cancer stem cells. J Med Chem 2019; 62: 964–86.
41. Gottesman MM, Fojo T, Bates SE. Multidrug resistance in cancer: role of ATP-dependent transporters. Nat Rev Cancer 2002; 2: 48–58.
42. Chen ZS, Tiwari AK. Multidrug resistance proteins (MRPs/ABCCs) in cancer chemotherapy and genetic diseases. FEBS J 2011; 278: 3226–45.
43. Grimm M, Krimmel M, Polligkeit J, et al. ABCB5 expression and cancer stem cell hypothesis in oral squamous cell carcinoma. Eur J Cancer 2012; 48: 3186–97.

Fig.1

Isolation and characterization of malignant pleural mesothelioma initiating cells. (a) Morphological analysis of adherent cells (AC) and initiating cells (IC)-enriched cultures derived from one epithelioid (Epi), one sarcomatous (Sar) and one biphasic (Bip) patient-derived malignant pleural mesothelioma (MPM), by contrast-phase microscope. Magnification: 20× objective lens (0.52 numerical aperture); 10× ocular lens. Bars: 100 µm. (b) Percentage of ALDHbright-positive cells, measured by flow cytometry, in AC and IC. Dot plots show one epithelioid MPM sample. Similar results were obtained on all the other MPM analyzed. The "+DEAB" condition was used to divide ALDHlow cells and ALDHbright cells, included in the R2 gate, as per manufacturer's instruction. R2 gate was then applied to the tested population ("-DEAB" condition). (c) Flow cytometry analysis of stemness markers Oct4, Nanog, SOX2 and ABCG2 in AC and IC epithelioid, sarcomatous and biphasic MPM. The histograms are representative of one patient per each histotype. (d) Self-renewal assay. AC and IC were diluted and seeded at a density of 1 cell/well; cells were counted weekly until day 48. Data are presented as means ± SD of all MPM samples (n = 3 experiments, 12 wells/sample). *p < 0.001: SC vs. IC (days 35–48). (e) Clonogenic assay. AC and IC were seeded at a density of 100 cells/well; the spheres or adherent colonies were counted weekly, until day 48. Data are presented as means ± SD of all MPM samples (n = 3 experiments, 6 wells/sample). *p < 0.001: IC vs. AC (days 35–48). (f) Heatmap of stemness-related genes in IC. The expression of each gene in the corresponding AC was considered 1 (not shown in the figure). The whole list of upregulated or downregulated genes is reported in the Supporting Information Table S4.

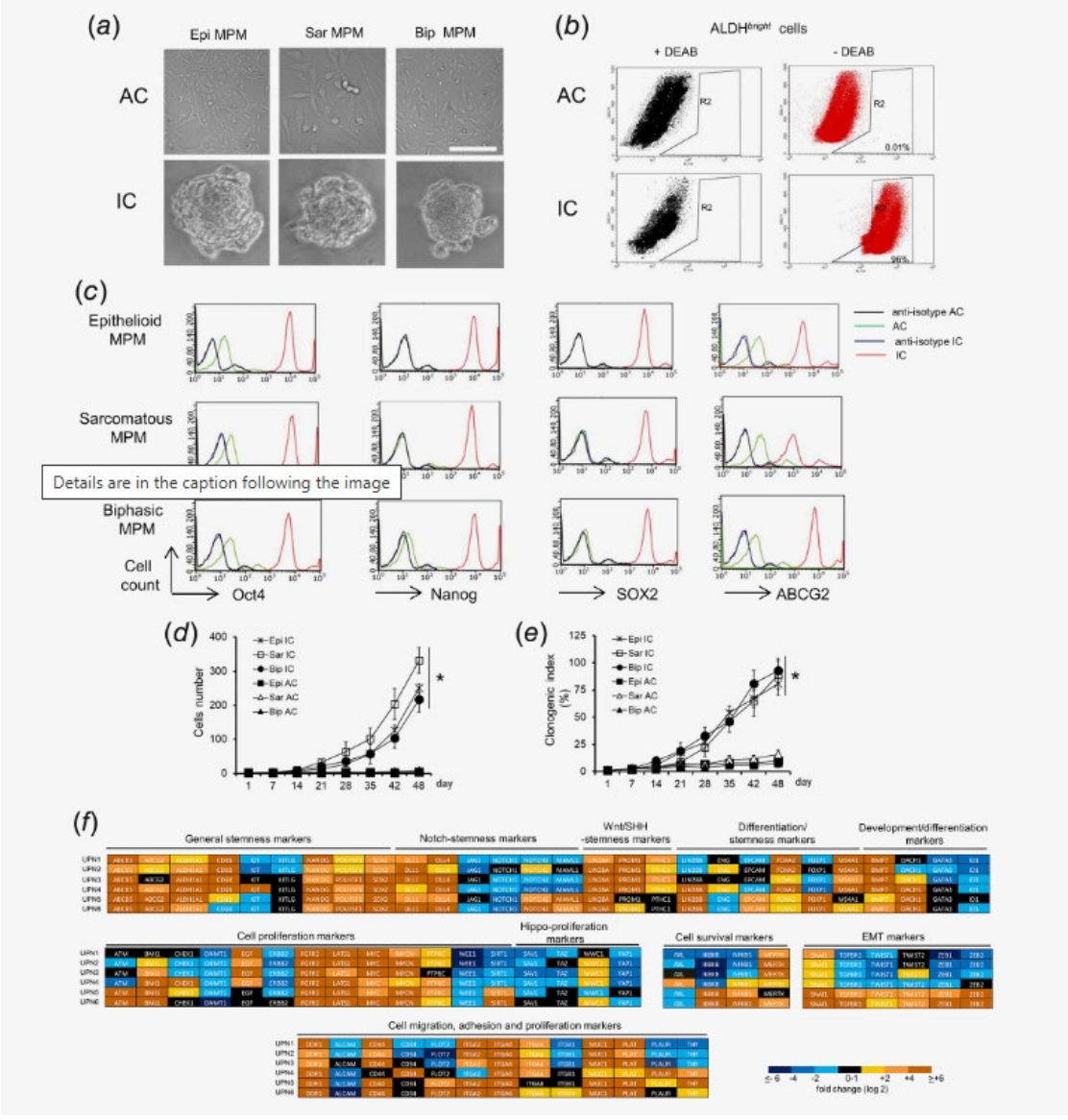

Fig.2

ABCB5 determines resistance to cisplatin and pemetrexed in malignant pleural mesothelioma initiating cells. AC and IC MPM were grown in fresh medium (ctrl), incubated with cisplatin (Pt, 25 µM) or pemetrexed (PMX, 5 µM). (a, b) Release of LDH, measured spectrophotometrically after 24 hr in duplicates, and cell viability, measured using a chemiluminescence-based method after 72 hr in quadruplicates. Data are presented as means ± SD of the pool of UPN 1–6. *p < 0.01: Pt/PMX-treated cells vs. ctrl cells; °p < 0.005: IC vs. AC. (c) ABCB5 mRNA as determined by qRT-PCR in triplicates. Data are presented as means ± SD of UPN 1–6 pool. *p < 0.001: IC vs. AC. (d) Representative immunofluorescence analysis of ABCB5. Green signal: ABCB5; blue signal: nuclear counterstaining with DAPI. Magnification: 63× objective lens (1.42 numerical aperture); 10× ocular lens. Bar: 20 µM. The micrographs are representative of one patient per each histotype. (e) Flow cytometry analysis of surface ABCB5 in AC and IC. The histograms are representative of one patient per each histotype. (f) IC from UPN1 (epithelioid MPM, epi) and UNP4 (sarcomatous MPM, sar) were transduced with a nontargeting scrambled vector (scr) or with a CRISPR/Cas9 ABCB5-knocking out vector (KO), lysed and immunoblotted with the indicated antibodies. The AC of the corresponding patients were used as internal control of cells lowly expressing ABCB5. The figure is representative of one out of three independent experiments. (g, h) The release of LDH was measured spectrophotometrically in duplicates, cell viability was measured using a chemiluminescence-based method in quadruplicates in UPN1 and UPN4 IC. Data are presented as means ± SD (n = 3). *p < 0.001: ABCB5-KO cells vs. scr-cells. (i) IC from UPN1 (epitelioid MPM) or UPN4 (sarcomatous MPM) were inoculated s.c. in 9 weeks old NOD-SCID-γ Balb/C female mice and treated as reported in the Materials and methods section. Data are means ± SD (n = 6/group). *p < 0.005: KO Pt + PMX vs. all the other groups (day 48). (j) Representative photos of tumors (day 48)

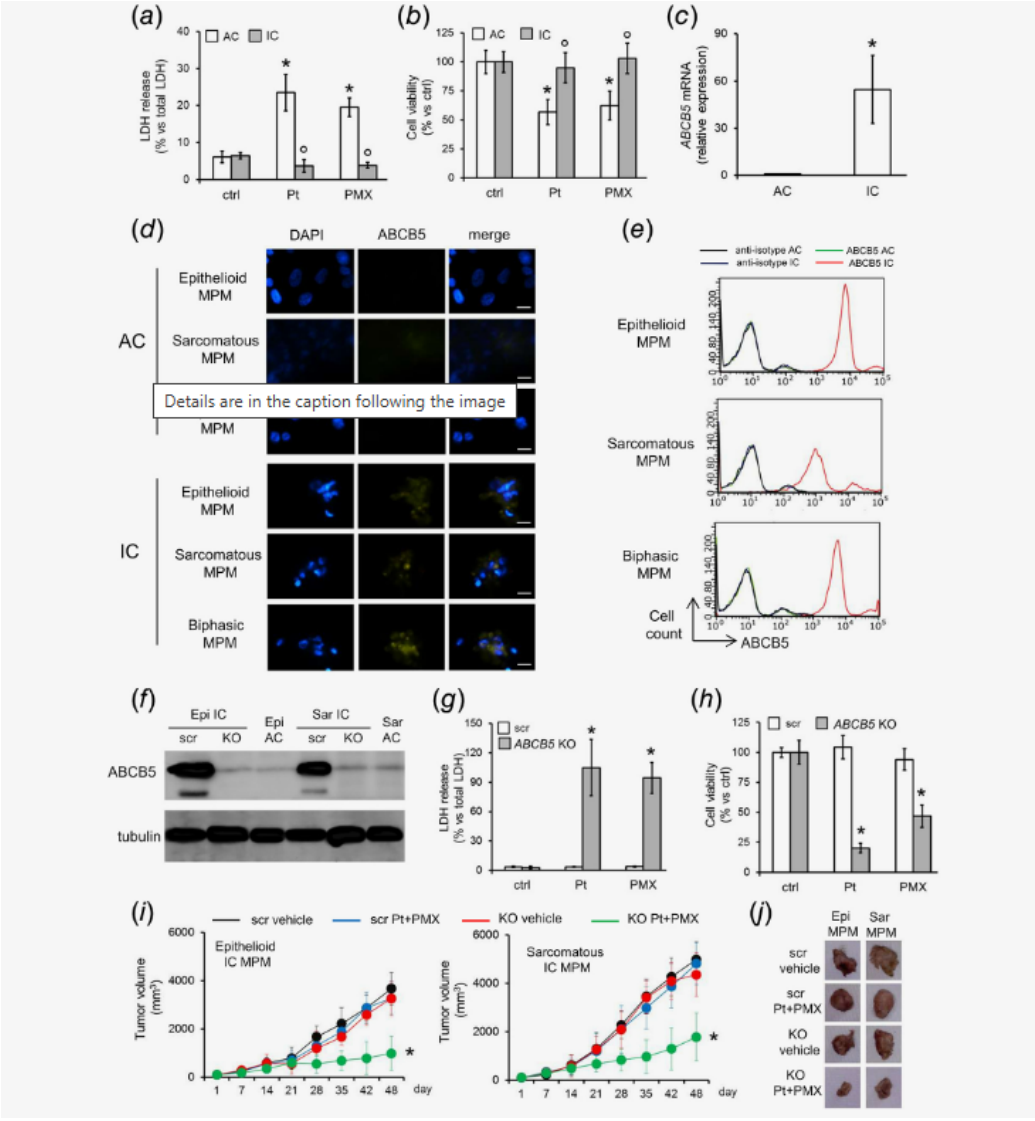

Fig. 3

ABCB5 knock-out prevents the acquisition of stemness properties in malignant pleural mesothelioma. (a) Adherent cells (AC) from epithelioid (UPN1) and sarcomatous (UPN4) malignant pleural mesothelioma (MPM) were transduced with a CRISPR/Cas9 ABCB5-knocking out (KO) vector, and selected for 6 weeks in the AC medium containing 1 μg/ml puromycin. After this period, cells were cultured for 2 weeks in the IC medium. This population was termed KO-ABCB5-AC and compared to parental AC, indicated as wild-type (wt) AC. IC-enriched cultures generated as reported in the Materials and methods section, untreated (wt-IC) or treated with a ABCB5 knocking-out vector (KO-ABCB5-IC), were used as reference. (b) ABCB5 mRNA as determined by qRT-PCR in triplicates. Data are presented as means ± SD (n = 3). *p < 0.001: wt-IC vs. wt-AC; °p < 0.001:KO-ACBC5-IC cells vs. KO-ACBC5-AC. (c) Morphological analysis of wt-IC, KO-ABCB5-AC and KO-ABCB5-IC after 2 weeks of culture in IC medium, by contrast-phase microscope. Magnification: 20× objective lens (0.52 numerical aperture); 10× ocular lens. Bars: 75 μm. (d) Flow cytometry analysis of stemness markers Oct4, Nanog, SOX2 and ABCG2 in wt-AC, KO-ABCB5-AC, wt-IC and KO-ABCB5-IC derived from UPN1 and UPN4. The histograms are representative of one out of three experiments. (e) Self-renewal assay. Cells were diluted and seeded at a density of 1 cell/well; cells were counted weekly until day 48. Data are presented as means ± SD (n = 3 experiments, 12 wells/sample). *p < 0.001: wt-IC vs. wt-AC; °p < 0.001: KO-ACBC5-IC cells vs. KO-ACBC5-AC. (f) Clonogenic assay. Cells were seeded at a density of 100 cells/well; the spheres or adherent colonies were counted weekly, until day 48. Data are presented as means ± SD (n = 3 experiments, 6 wells/sample). *p < 0.001: wt-IC vs. wt-AC; °p < 0.001:KO-ACBC5-IC cells vs. KO-ACBC5-AC.

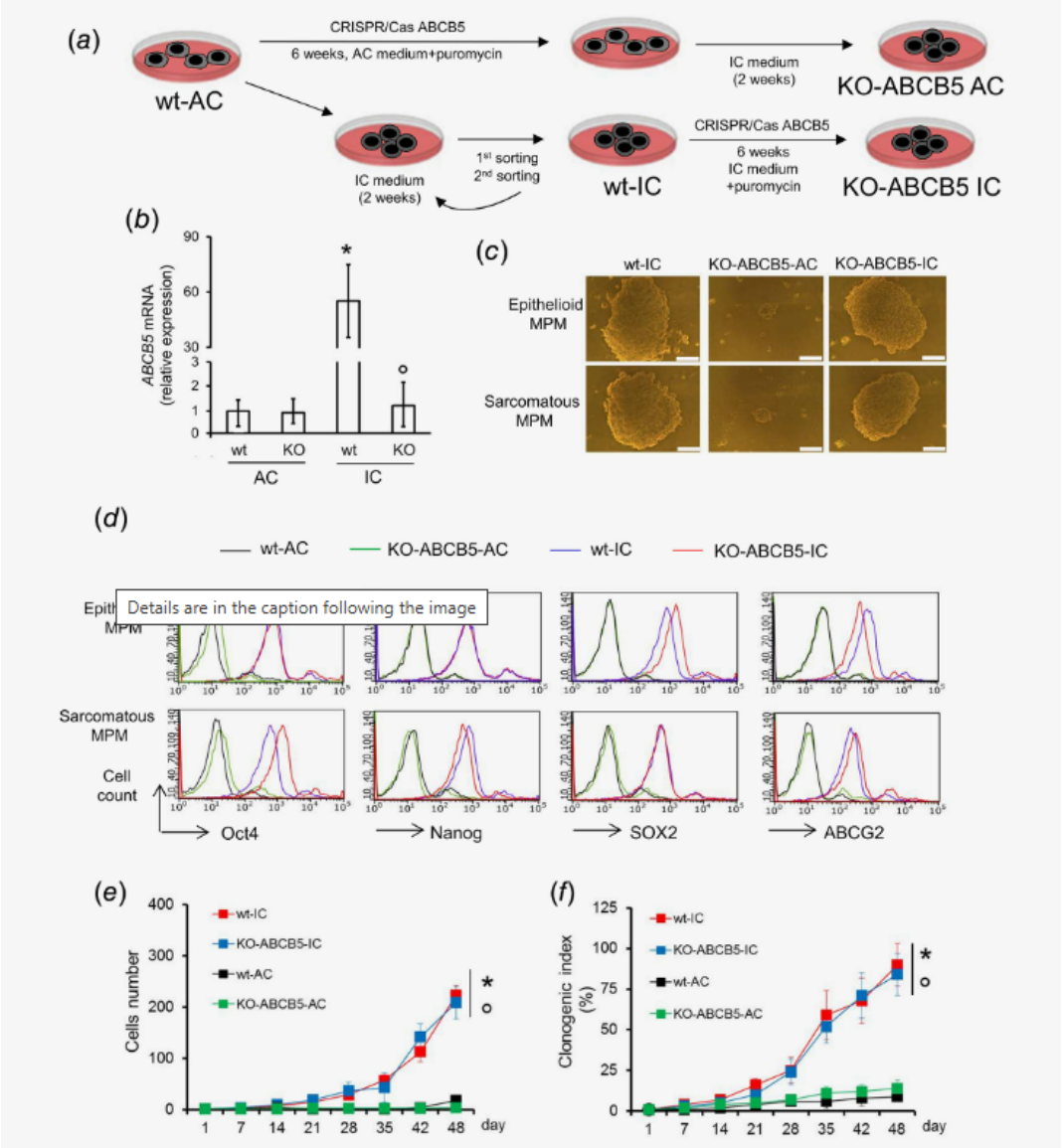

Fig. 4

Malignant pleural mesothelioma initiating cells have Wnt canonical pathway constitutively upregulated. (a) Heatmap of Wnt pathway-related genes in epithelioid (Epi), sarcomatous (Sar) and biphasic (Bip) IC. The expression of each gene in the corresponding AC was considered 1 (not shown in the figure). The whole list of upregulated or downregulated genes is reported in Supporting Information Table S6. (b) Flow cytometry analysis of Wnt receptors Frizzled 1, Frizzled 2, Frizzled 3 and coreceptor LRP6 in MPM AC and IC. The histograms are representative of one epithelioid (Epi, UPN1) and sarcomatous (Sar, UPN4) patient. Similar results were obtained in all the other MPM analyzed. (c) Immunoblot analysis of phospho(Tyr279/Tyr216)GSK3 (pGSK3β), GSK3β, phospho(Ser33/Ser37/Thr41)-β-catenin (pβ-cat), β-catenin (β-cat) in whole-cell lysates of epithelioid (UPN1) and sarcomatous (UPN4) AC and IC. The β-tubulin expression was used as a control of equal protein loading. Similar results were obtained in all the other MPM analyzed. (d) Whole-cell lysates of epithelioid (UPN1) and sarcomatous (UPN4) AC and IC were immunoprecipitated (IP) with an anti-β-catenin (β-cat) antibody, then immunoblotted (IB) with an antimono/polyubiquitin (UB) antibody. The β-tubulin expression was used as a control of equal protein loading. Similar results were obtained in all the other MPM analyzed. no Ab: Epi AC sample immunoprecipitated without anti-β-catenin antibody. (e) The cytosolic and nuclear extracts from epithelioid (UPN1) and sarcomatous (UPN4) AC and IC were analyzed for the amount of β-catenin (β-cat). The expression of β-tubulin and TBP were used as a controls of equal protein loading in cytosolic and nuclear fractions. The figure is representative of one out of three experiments with similar results.

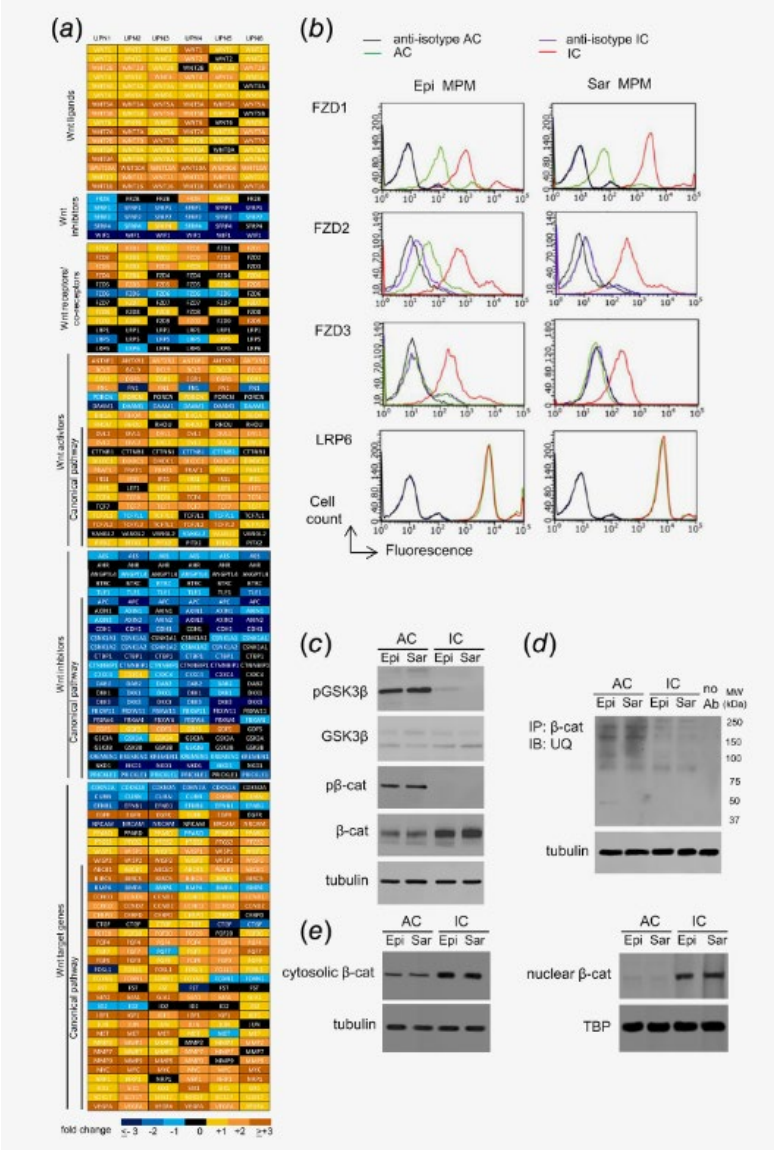

Fig. 5

ABCB5 is controlled by Wnt/GSK3β/β-catenin/c-myc pathway. AC and IC were grown in fresh medium (ctrl). When indicated, AC were treated for 6 hr (panels a and b) or 24 hr (panels c and d) with the Wnt pathway activator (i.e., GSK3β inhibitor) LiCl (10 mM), IC were treated with the c-myc inhibitor 5-[(4-ethylphenyl)methylene]-2-thioxo-4-thiazolidinone (myc-i, 250 µM). (a) Representative immunofluorescence analysis of c-myc in AC and IC MPM cells from UPN1, grown in fresh medium (ctrl). Red signal: c-myc; blue signal: nuclear counterstaining with DAPI. Magnification: 63× objective (1.42 numerical aperture); 10× ocular lens. Bar: 20 µM. Similar results were obtained in all the other MPM analyzed. (b) Binding of c-myc to the ABCB5 promoter, measured by ChIP in triplicates. Data are presented as means ± SD of UPN 1–6 pool. *p < 0.02: LiCl-treated/myc-i-treated cells vs. ctrl cells; °p < 0.02: IC vs. AC. (c) Levels of ABCB5 mRNA as determined by qRT-PCR in triplicates. Data are presented as means ± SD of UPN 1–6 pool. *p < 0.005: LiCl/myc-i-treated cells vs. ctrl cells; °p < 0.001: IC vs. AC. (d). Cells treated as indicated above were grown in the absence (ctrl) or in the presence of cisplatin (Pt, 25 µM) or pemetrexed (PMX, 5 µM). The release of LDH was measured spectrophotometrically, in duplicates. Data are presented as means ± SD of UPN 1–6 pool. *p < 0.001: Pt/PMX-treated AC vs. ctrl cells; °p < 0.001: Pt/PMX-treated IC vs. Pt/PMX-treated AC; #p < 0.005: LiCl-treated or myc-i-treated, Pt/PMX-treated AC vs. Pt/PMX-treated AC or IC, respectively.

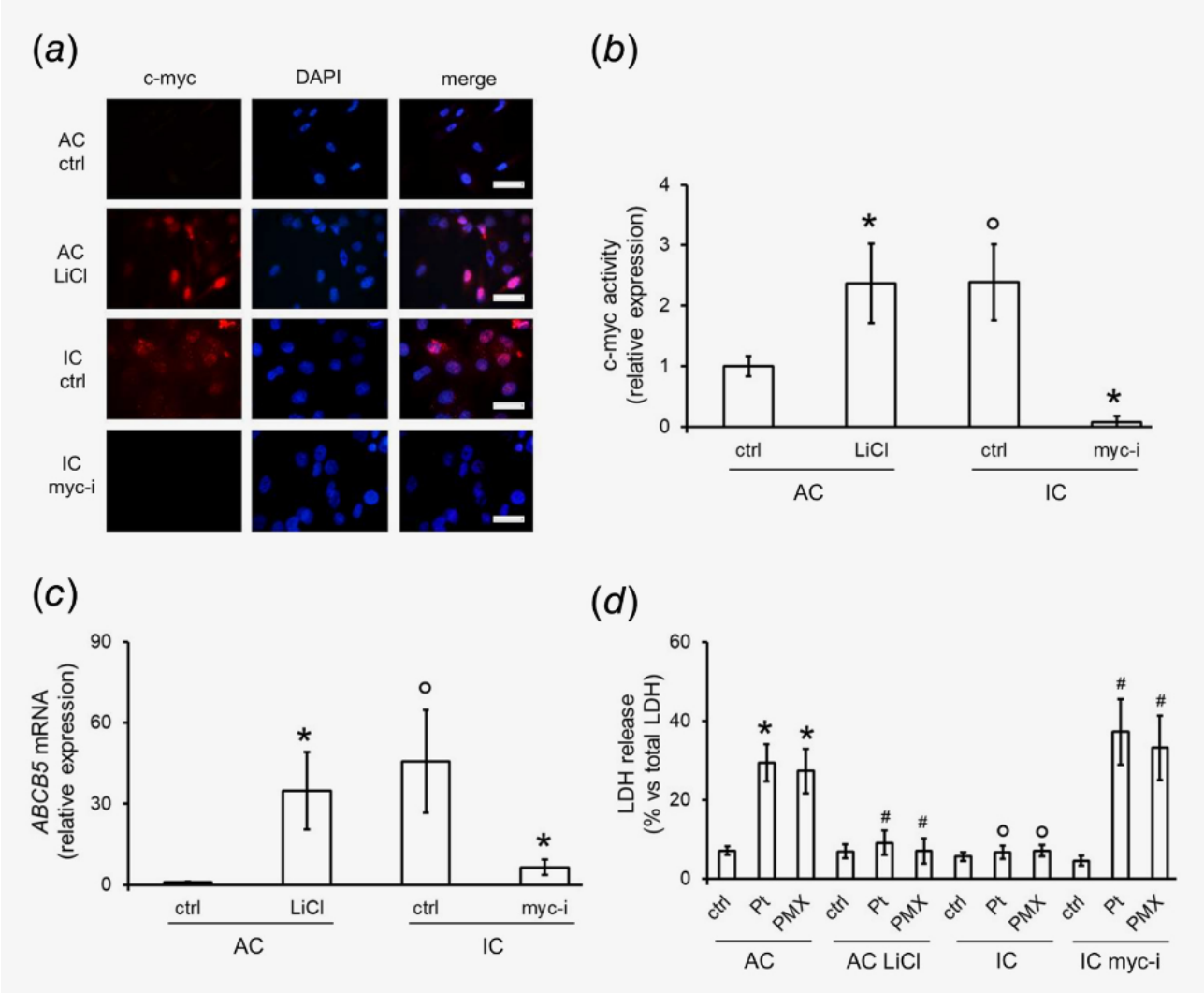

Fig. 6

IL-8 and IL-1β contribute to ABCB5-mediated resistance in malignant pleural mesothelioma initiating cells. (a) Relative expression of cytokine mRNAs in IC vs. AC MPM, measured by qRT-PCR array. Data are presented as means ± SD of the pool of UPN 1–6 IC. (b, c) mRNA levels of IL-8 or IL-1β assessed by qRT-PCR, in triplicates, in IC transfected with a nontargeting scrambled vector (scr) or with a CRISPR/Cas9 IL-8- or IL-1β-knocking-out (KO) vector. AC (−) were included as reference. Data are presented as means ± SD of UPN 1–6 pool. *p < 0.002: scr-IC vs. AC; °p < 0.001: KO-IC vs. scr-IC. (d, e) IL-8 or IL-1β production, measured by ELISA, in duplicates. Data are presented as means ± SD of UPN 1–6 pool. *p < 0.05: scr-IC vs. AC; °p < 0.001: KO-IC vs. scr-IC. (f, g) IL-8 or IL-1β production, measured by ELISA in duplicates, in AC and IC. MPM cells were grown for 24 hr in fresh medium (ctrl), treated with the GSK3β inhibitor (i.e., Wnt pathway activator) LiCl (10 mM) or the c-myc inhibitor 5-[(4-ethylphenyl)methylene]-2-thioxo-4-thiazolidinone (myc-i, 250 μM). Data are presented as means ± SD of UPN 1–6 pool. *p < 0.02: LiCl-treated AC/ctrl IC vs. ctrl-AC; °p < 0.001:myc-i-treated IC vs. ctrl-IC. (h) Binding of c-myc to the ABCB5 promoter, measured by ChIP, in triplicates. Data are presented as means ± SD of UPN 1–6 pool. *p < 0.02: scr-IC vs. AC; °p < 0.05: KO-IC vs. scr-IC. (i) Levels of ABCB5 mRNA as determined by qRT-PCR, in triplicates. Data are presented as means ± SD of UPN 1–6 pool. *p < 0.001: scr-IC vs. AC; °p < 0.01: KO-IC vs. scr-IC. (j) SC were grown in fresh medium (24 hr) or in medium containing cisplatin (Pt, 25 μM) or pemetrexed (PMX, 5 μM). The release of LDH was measured spectrophotometrically, in duplicates. Data are presented as means ± SD of UPN 1–6 pool. *p < 0.005: Pt/PMX-treated IL-8 KO/IL-1β KO-cells vs. untreated (ctrl) KO-cells; °p < 0.002: Pt/PMX-treated IL-8 KO/IL-1β KO-cells vs. Pt/PMX-treated scr-cells. (k) Proposed mechanisms of the multiple autocrine loops upregulating ABCB5 and determining resistance to cisplatin and pemetrexed in MPM IC.

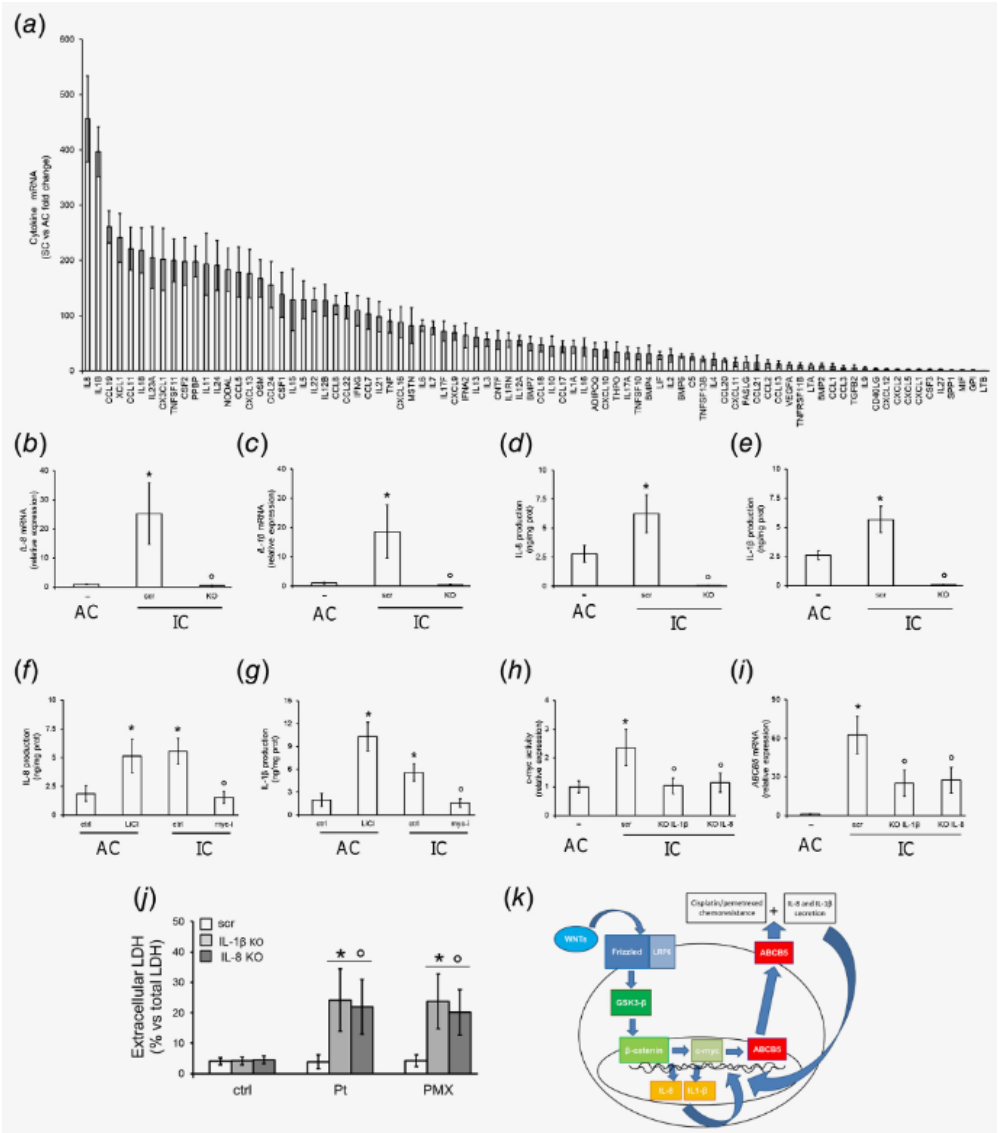

Fig. 7

ABCB5 is a negative prognostic factor in malignant pleural mesothelioma patients. (a, b) Representative immunohistochemistry images of ABCB5-positive cells within MPM (panel a): 60×, bar: 100 µm; (panel b): 100×, bar: 100 µm). Arrow: ABCB5-strongly positive cells. (c, d) ABCB5 staining was ranked according to staining extent of each patient (Supporting Information Table S7), and median value was calculated. Patients were classified as ABCB5^{low} and ABCB5^{high} if the staining was low or equal/higher than the median value. Time to progression (panel c), for the patients with available data, and overall survival (panel d) probability was calculated using the Kaplan–Meier method. *p < 0.005 (panel c); *p < 0.05 (panel d): ABCB5 ^{high} vs. ABCB5 ^{low} group.

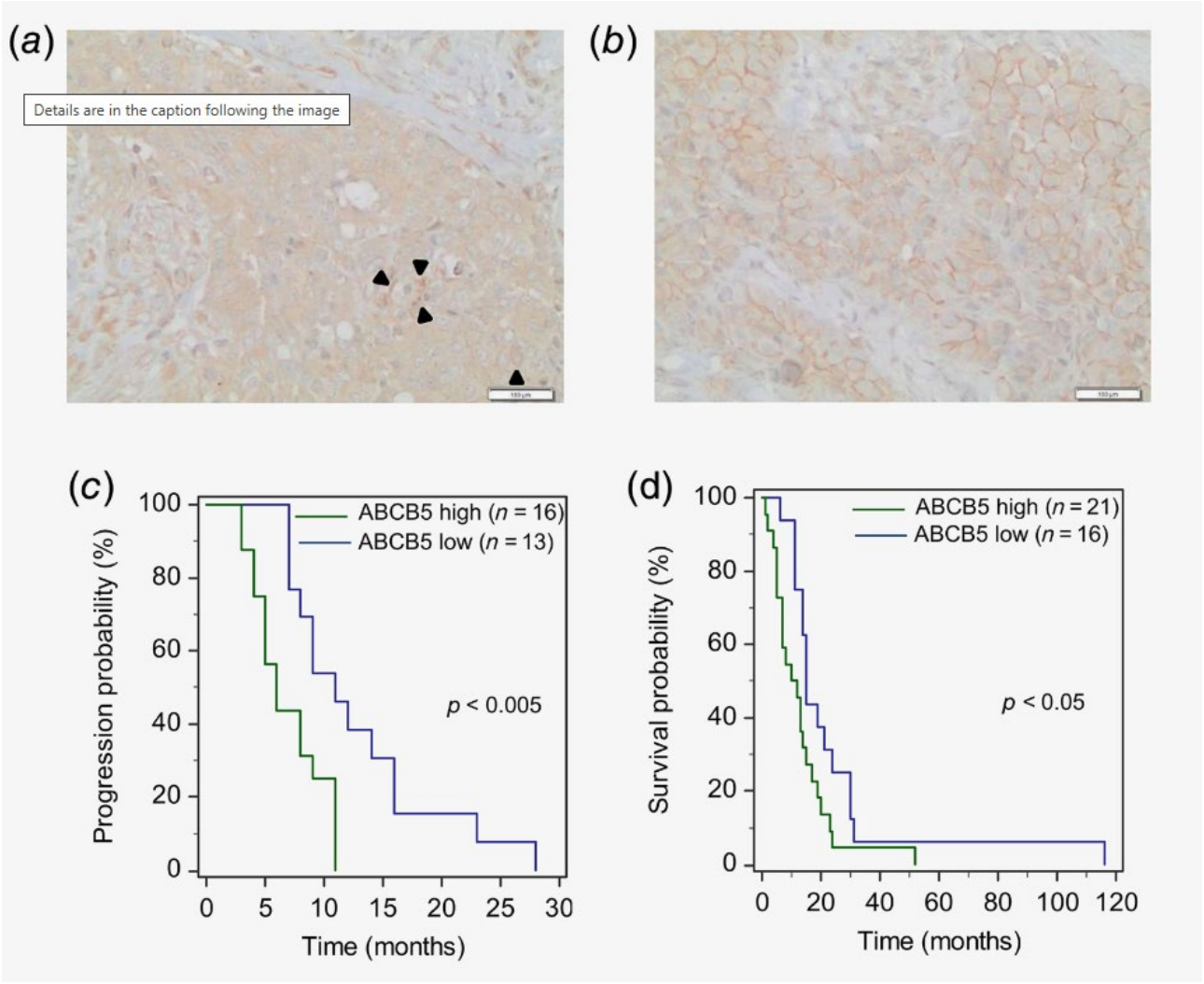

Supplementary materials

Supplementary Figure legends

Supplementary Figure S1

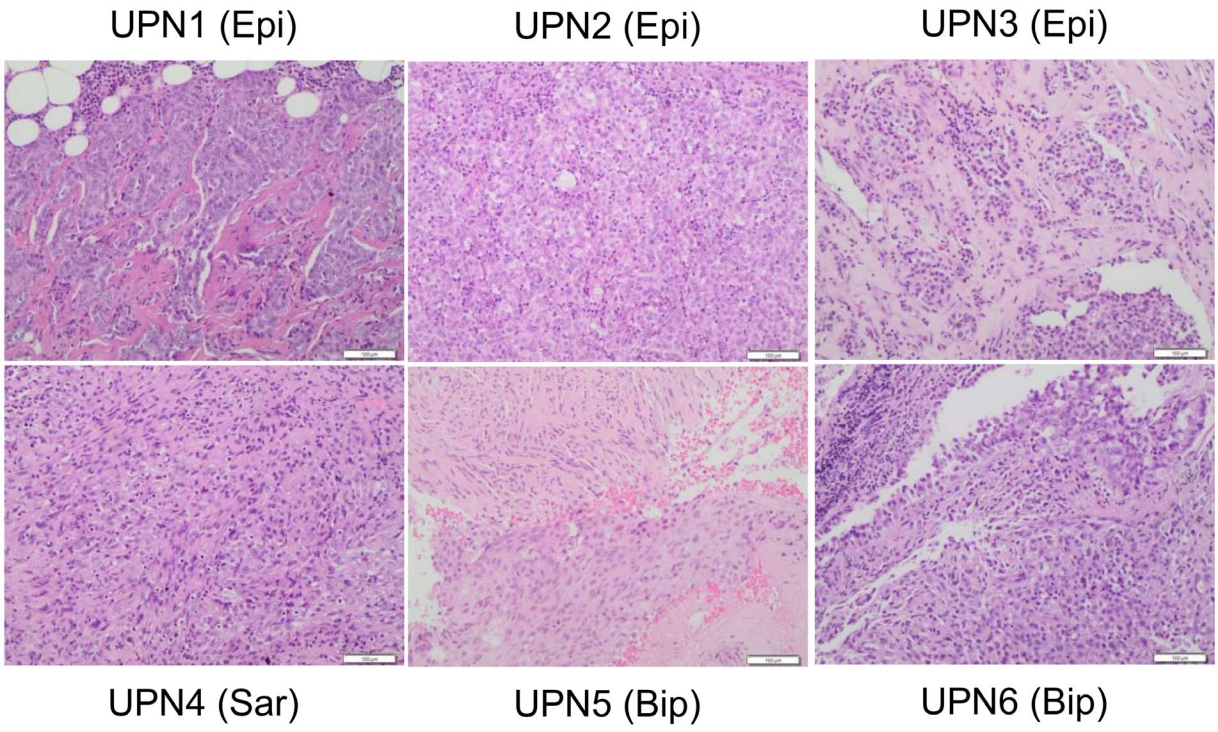

Supplementary Figure S1. Representative histology images of UPN 1-6

Representative original MPM specimen histological images of UPN1-6 samples (hematoxilin and eosin, 10×, bar: 100 μm). Epi: epithelioid; Sar: sarcomatous; Bip: biphasic.

Supplementary Figure S2

	Pt	PMX
UPN1	IC_{50} Pt (AC): 20.96 ± 2.34 µM IC_{75} Pt (AC): 48.79 ± 5.91 µM IC_{50} PMX (AC): 4.02 ± 2.86 µM IC_{75} PMX (AC): 17.53 ± 1.58 µM	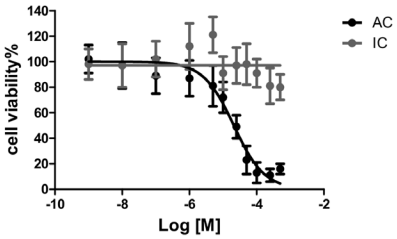 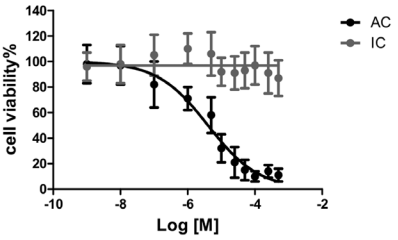
UPN2	IC_{50} Pt (AC): 7.99 ± 1.53 µM IC_{75} Pt (AC): 33.15 ± 5.01 µM IC_{50} PMX (AC): 2.20 ± 0.47 µM IC_{75} PMX (AC): 9.17 ± 1.86 µM	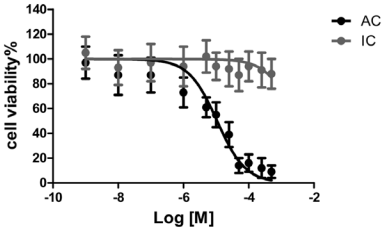 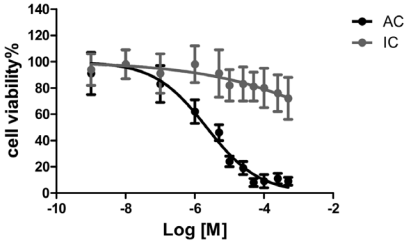
UPN3	IC_{50} Pt (AC): 20.74 ± 2.09 µM IC_{75} Pt (AC): 47.14 ± 8.21 µM IC_{50} PMX (AC): 4.95 ± 1.17 µM IC_{75} PMX (AC): 22.08 ± 3.41 µM	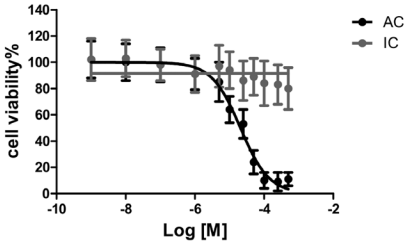 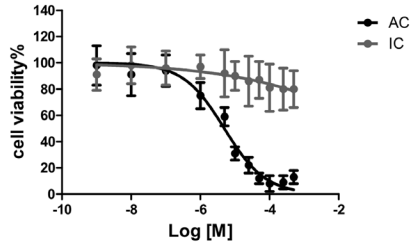
UPN4	IC_{50} Pt (AC): 24.87 ± 1.28 µM IC_{75} Pt (AC): 69.27 ± 6.51 µM IC_{50} PMX (AC): 4.92 ± 0.27 µM IC_{75} PMX (AC): 19.25 ± 2.39 µM	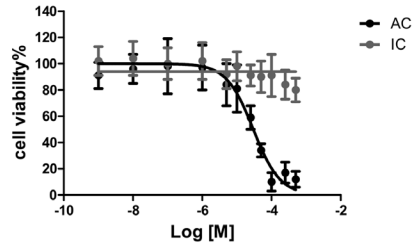 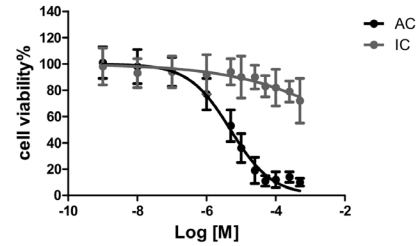
UPN5	IC_{50} Pt (AC): 18.80 ± 2.83 µM IC_{75} Pt (AC): 75.29 ± 8.94 µM IC_{50} PMX (AC): 2.72 ± 1.17 µM IC_{75} PMX (AC): 9.82 ± 1.74 µM	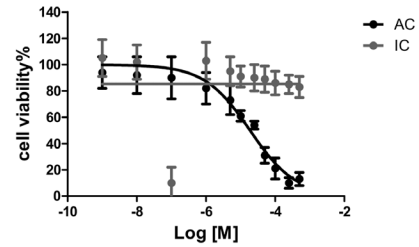 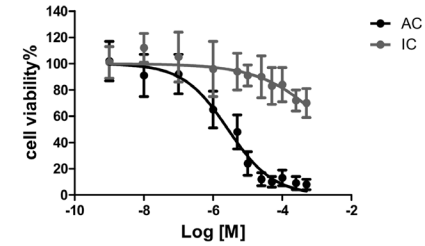
UPN6	IC_{50} Pt (AC): 11.51 ± 1.39 µM IC_{75} Pt (AC): 68.52 ± 7.19 µM IC_{50} PMX (AC): 4.87 ± 1.25 µM IC_{75} PMX (AC): 26.04 ± 2.55 µM	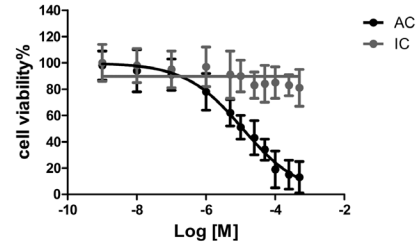 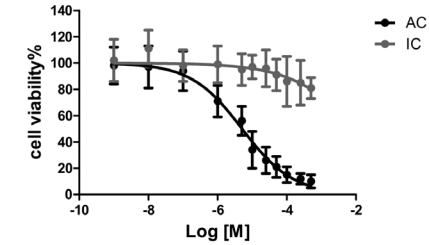

Supplementary Figure S2. Dose-response viability experiments

AC and IC were incubated 72 h with increasing concentrations (1 nM, 10 nM, 100 nM, 1 μM, 5 μM, 10 μM, 25 μM, 50 μM, 100 μM, 250 μM, 500 μM) of cisplatin and pemetrexed. Cell viability was measured using a chemiluminescence-based method after 72 h in quadruplicates. IC_{50} and IC_{75} were defined as the concentrations of each drug that reduced viability to 50% and 25 % compared to untreated cells, producing 50% and 75% cell death, respectively

Supplementary Figure S3

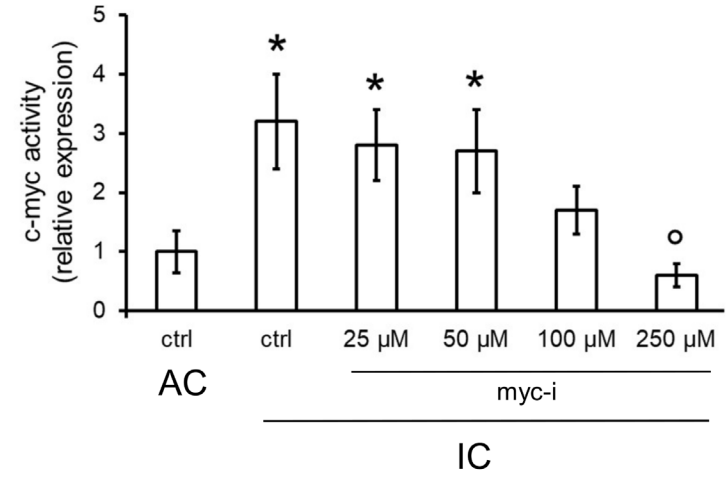

Supplementary Figure S3. Dose-response inhibition of c-myc transcriptional activity

AC and IC were grown in fresh medium (ctrl). When indicated, IC were treated for 6 h with the with the c-myc inhibitor 5-[(4-Ethylphenyl)methylene]-2-thioxo-4-thiazolidinone (myc-i) at 25, 50, 100 and 250 µM. The binding of c-myc to the *ABCB5* promoter was measured by ChIP, in triplicates. Data are presented as means±SD of UPN 1-6 pool. *$p<0.005$: IC vs AC; °$p<0.001$: myc-i-treated cells vs ctrl.

Supplementary Figure S4

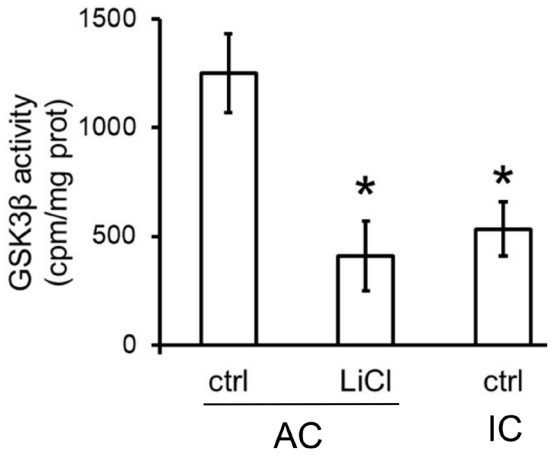

Supplementary Figure S4. Inhibition of LiCl on GSK3β activity

AC and IC were grown in fresh medium (ctrl). When indicated, AC were treated for 6 h with the GSK3β inhibitor LiCl (10 mM). GSK3β activity was immuno-purified from cell extracts and the activity was measured by a radiometric assay in duplicates. Data are presented as means±SD of UPN 1-6 pool. *p<0.001:LiCl-treated AC/untreated IC vs ctrl AC.

Supplementary Figure S5

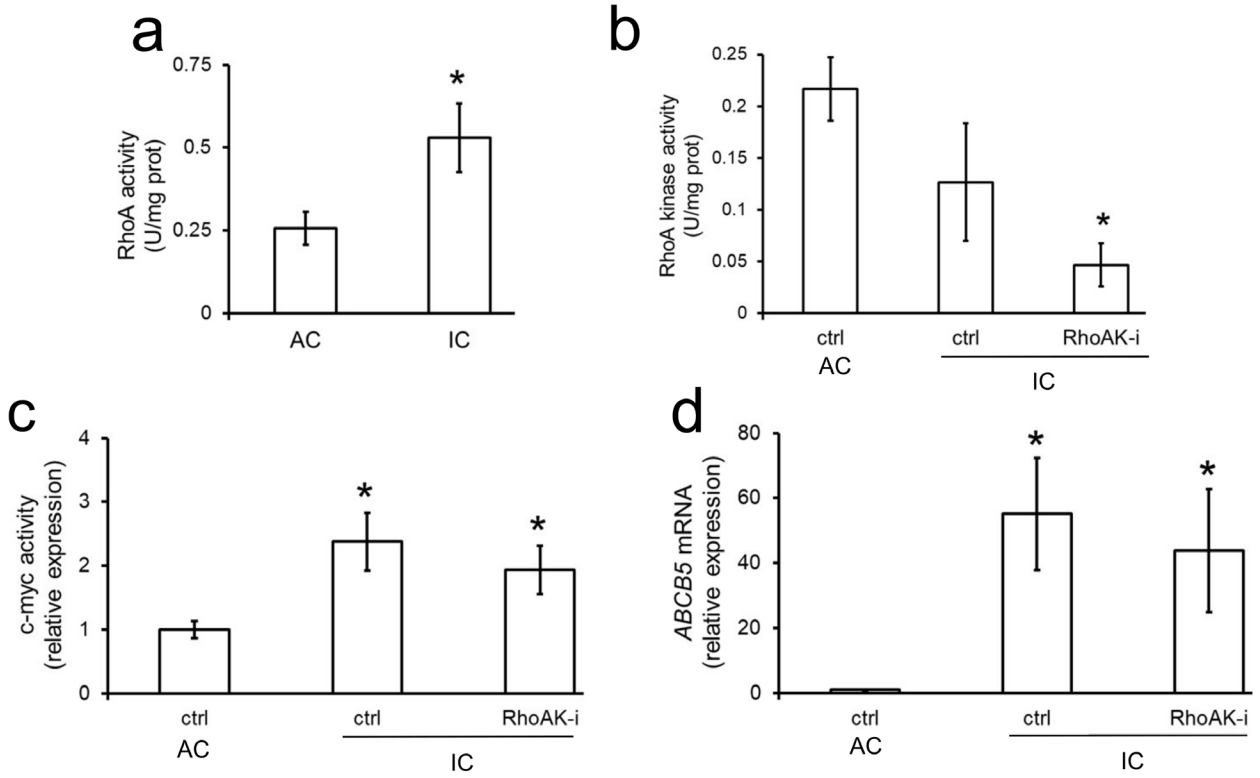

Supplementary Figure S5. Effects of RhoA/RhoA kinase pathway on c-myc activity and ABCB5 transcription

AC and IC were grown in fresh medium (ctrl). When indicated, IC were treated for 24 h with the RhoA kinase inhibitor Y27632 (10 µM; RhoAK-i). **a-b.** Rho-GTP bound fraction, an index of active RhoA, and RhoA kinase activity were measured by ELISA, in duplicates. Data are presented as means±SD of UPN 1-6 pool. *p<0.01:IC vs AC. **c**. Binding of c-myc to the *ABCB5* promoter, measured by ChIP, in triplicates. Data are presented as means±SD of UPN 1-6 pool. *p<0.005:IC vs AC. **d.** Levels of *ABCB5* mRNA as determined by qRT-PCR in triplicates. Data are presented as means±SD of UPN 1-6 pool. *p<0.001:IC vs AC.

Supplementary Figure S6

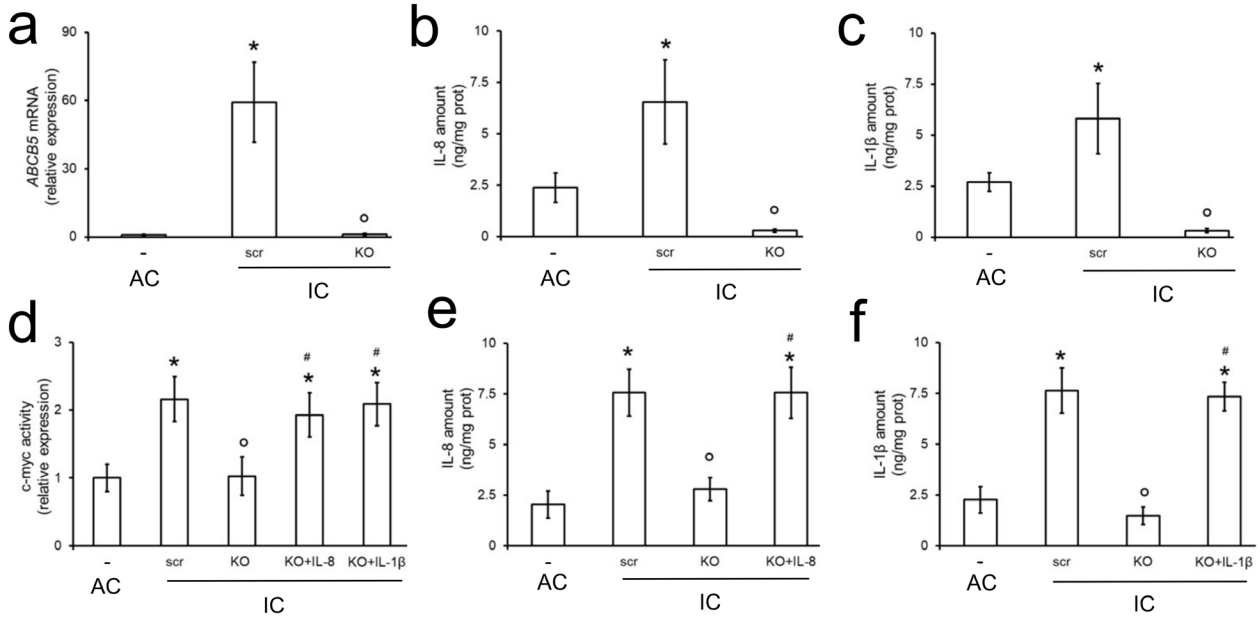

Supplementary Figure S6. Effects of *ABCB5* knock-out on IL-8 and IL-1β secretion, and c-myc transcriptional activity

a. IC were transduced with a non-targeting scrambled vector (scr) or with a CRISPR/Cas9 *ABCB5*-knocking-out (KO) vector. AC (-) were used as internal control of ABCB5 lowly expressing cells. Levels of *ABCB5* mRNA as determined by qRT-PCR in triplicates. Data are presented as means±SD of UPN 1-6 pool. *p<0.001:scr-IC vs AC; °p<0.001:KO-IC vs scr-IC. **b-c**. Amount of IL-8 or IL-1β in the supernatants measured by ELISA in duplicates. Data are presented as means±SD of UPN 1-6 pool. *p<0.05:scr-IC vs AC; °p<0.001:KO-IC vs scr-IC. **d.** Binding of c-myc to the *ABCB5* promoter, measured by ChIP in triplicates. When indicated, KO-IC were incubated with 100 ng/mL IL-8 or IL-1β, 24 h before ChIP experiment. Data are presented as means±SD of UPN 1-6 pool. *p<0.002: IC vs AC; °p<0.005: KO-IC vs scr-IC; $^{\#}$p<0.002: KO+IL-8/IL-1β-IC vs KO-IC. **e-f**. Amount of IL8 or IL-1β in the supernatants, measured by ELISA in duplicates. Data are presented as means±SD of UPN 1-6 pool. *p<0.001:IC vs AC; °p<0.001: KO-IC vs scr-IC; $^{\#}$p<0.001: KO+IL-8/IL-1β-SC vs KO-IC.

Supplementary Tables

Supplementary Table S1. Clinical features of patients

MPM (UPN)	Histotype	Sex	Age (years)	Asbestos exposure	Surgery	Radiotherapy	First-line treatment	Second-line treatments	PFS (months)	OS (months)
1	epithelioid	M	51	P	No	No	Cisplatin+pemetrexed	Gemcitabine Vinorelbine	4.1	23
2	epithelioid	M	77	P	No	Yes	Cisplatin+pemetrexed	Gemcitabine	10.3	16
3	epithelioid	F	47	E	No	Yes	Cisplatin+pemetrexed	Trabectedin	5	12
4	sarcomatous	M	69	E	No	No	Cisplatin+pemetrexed	Trabectedin	2.6	10
5	biphasic	M	64	P	No	No	Cisplatin+pemetrexed	Cisplatin +pemetrexed	5.5	16
6	biphasic	M	72	P	No	No	Cisplatin+pemetrexed	Trabectedin	5.1	21

Histological classification of MPM samples, anagraphic and clinical data of patients. M: male; F: female; P: professional; E: environmental; U: unlikely; ND: not-determined. UPN: unknown patient number. PFS: progression free survival: survival with stable disease from the beginning of cisplatin therapy. OS: overall survival: survival from the beginning of cisplatin therapy until patients exitus.

Supplementary Table S2. Histological characterization of mesothelioma samples

MPM (UPN)	CALR	PANCK	POD	EMA	CEA	WT1	CK5
1	POS	POS	NEG	NEG	NEG	POS	NEG
2	POS	POS	NEG	NEG	NEG	POS	NEG
3	POS	POS	NEG	POS	NEG	POS	NEG
4	FOC	FOC	NEG	NEG	NEG	FOC	NEG
5	POS	POS	NEG	NEG	NEG	NEG	NEG
6	POS	POS	NEG	NEG	NEG	FOC	NEG

Results of the immunohistochemical staining of MPM samples for calretinin (CALR), pancytokeratin (PANCK), podoplanin (POD), epithelial membrane antigen (EMA), carcino-embryonic antigen (CEA), Wilms tumor-1 antigen (WT1), cytokeratin 5 (CK5). POS: positive; NEG: negative; FOC: focal positivity. UPN: unknown patient number.

Supplementary Table S3. *In vivo* tumorigenicity assay

Tumor type	Tumor number	Tumor volume (mm^3)	Euthanasia (week)
Epi AC	0/9	na	30
Sar AC	0/9	na	30
Bip AC	1/9	580 ± 98	30
Epi IC	8/9	4523 ± 952	14 ± 2
Sar IC	5/9	5987 ± 1168	11 ± 3
Bip IC	6/9	5069 ± 997	10 ± 2

1×10^8 AC or IC (3 mice for each patient-derived AC or IC sample; 9 mice/group), were injected subcutaneously (s.c.) in 6-week-old female NOD-SCID-γ Balb/C mice. Tumor growth was measured daily by caliper, according to the equation $(LxW^2)/2$, where L=tumor length and W=tumor width, up to 30 weeks. Mice bearing AC tumors were euthanized at week 30; mice bearing IC tumors were euthanized in case of: 1) tumor ulceration; 2) tumor volume >8000 mm^3; 3) weight reduction >20%. Tumor number: number of tumors developed/group at the time of euthanasia. Tumor volume: mean volume±SD at the time of euthanasia. All formed tumors were positive for calretinin and pancytokeratin, considered markers of MPM.

Supplementary Table S4. Expression of stemness-related genes in malignant pleural mesothelioma cells

Ref Seq	Gene name	Biological function	Fold change (epi SC vs epi AC)	p value	Fold change (sar SC vs sar AC)	p value	Fold change (bip SC vs bip AC)	p value
NM_000007.13	ABCB5	Stemness marker	5.73	0.022	4.21	0.022	5.31	0.001
NM_000004.11	ABCG2	Stemness marker	2.79	0.035	2.02	0.048	7.01	0.0018
NM_000009.11	ALDH1A1	Stemness marker	4.18	0.001	5.93	0.0054	4.88	0.0022
NM_000004.11	CD38	Stemness marker	12.00	0.001	6.515	0.008	0.91	ns
NM_000004.11	KIT	Stemness marker; cell proliferation	0.37	ns	9.883	0.043	0.56	0.035
NM_000012.11	KITLG	Stemness marker	0.24	0.049	0.78	ns	0.83	ns
NM_000012.11	NANOG	Stemness marker	5.07	0.001	7.78	0.0023	7.89	0.0022
NM_000006.11	POU5F1	Stemness marker	3.53	0.013	2.928	0.0038	6.12	0.007
NM_000003.11	SOX2	Stemness marker	4.72	0.001	8.01	0.0005	9.29	0.0024
NM_000006.11	DLL1	Stemness/differentiation marker; Notch ligand	7.96	0.001	1.51	ns	6.21	0.029
NM_000015.9	DLL4	Stemness/differentiation marker; Notch ligand	3.63	0.042	15.23	0.0021	7.18	0.0019
NM_000020.10	JAG1	Stemness/differentiation marker; Notch ligand	0.38	0.009	0.32	0.0019	0.99	ns
NM_000009.11	NOTCH1	Stemness/differentiation marker; Notch signalling	0.78	ns	0.69	ns	0.27	0.0015
NM_000001.10	NOTCH2	Stemness/differentiation marker; Notch signalling	1.40	ns	0.39	0.029	7.67	0.041
NM_000005.9	MAML1	Development; Notch signalling	0.19	0.001	0.37	0.0019	8.44	0.0023
NM_000001.10	LIN28A	Development; Wnt/Sonic Hedgehog signalling	6.11	0.001	10.01	0.0027	8.34	0.0018
NM_000004.11	PROM1	Stemness/differentiation marker; Wnt/Sonic Hedgehog signalling	10.52	0.001	7.01	0.0036	1.49	0.081
NM_000009.11	PTCH1	Stemness/differentiation marker; Hedgehog signalling	3.58	0.0013	2.56	0.043	1.43	ns
NM_000006.11	LIN28B	Stemness/differentiation marker	0.53	ns	3.81	0.0042	8.09	0.0016
NM_000009.11	ENG	Stemness/differentiation marker	1.05	ns	2.18	0.0039	0.78	ns
NM_000002.11	EPCAM	Stemness/differentiation marker; cell adhesion	0.61	ns	0.29	0.041	4.88	0.0028
NM_000020.10	FOXA2	Stemness/differentiation marker	6.29	0.001	4.34	0.001	0.93	ns
NM_000003.11	FOXP1	Stemness/differentiation marker	0.45	0.001	0.17	0.0011	6.41	0.028
NM_000011.9	MS4A1	Development; differentiation marker	4.73	0.0037	5.13	0.0029	1.01	ns
NM_000020.10	BMP7	Development	10.32	0001	4.33	0.0028	2.9	0.0027
NM_000013.10	DACH1	Development	1.01	ns	4.17	0.0018	13.56	0.0009
NM_000010.10	GATA3	Differentiation marker	0.33	0.009	0.91	ns	1.23	ns
NM_000020.10	ID1	Differentiation marker	0.34	0.0037	0.27	0.021	0.81	ns

NM_000011.9	ATM	Cell proliferation; DNA damage	0.89	ns	1.29	ns	4.41	0.023
NM_000010.10	BMI1	Cell proliferation; DNA damage; chromatin remodelling	1.92	ns	2.81	ns	6.53	0.0017
NM_000011.9	CHEK1	Cell proliferation; DNA damage	0.35	0.013	4.12	0.0039	1.29	ns
NM_000019.9	DNMT1	Cell proliferation; chromatin remodelling	0.41	0.0044	0.37	0.0021	0.09	0.0012
NM_000004.11	EGF	Cell proliferation	6.88	0.009	3.11	0.039	0.62	0.039
NM_000017.10	ERBB2	Cell proliferation	0.49	ns	0.17	0.0021	0.97	ns
NM_000010.10	FGFR2	Cell proliferation	10.68	0.0012	10.01	0.0009	7.27	0.0018
NM_000006.11	LATS1	Cell proliferation	6.02	0.0025	11.39	0.0002	6.73	0.0009
NM_000008.10	MYC	Cell proliferation	14.10	0.001	2.98	0.038	7.12	0.0082
NM_000002.11	MYCN	Cell proliferation	6.92	0.0012	2.81	0.013	7.01	0.0023
NM_000001.10	PTPRC	Cell proliferation	1.58	ns	5.11	0.0037	4.91	0.0003
NM_000011.9	WEE1	Cell proliferation	0.51	0.0014	0.26	0.0018	0.45	0.0034
NM_000010.10	SIRT1	Cell proliferation; DNA damage; chromatin remodelling	0.34	0.024	0.31	0.0024	6.01	0.0003
NM_000014.8	SAV1	Cell proliferation; cell migration; Hippo signalling	0.27	0.009	0.71	ns	0.73	ns
NM_000023.10	TAZ	Cell proliferation; Hippo signalling	0.51	ns	0.47	0.049	1284	ns
NM_000005.9	WWC1	Cell proliferation; Hippo signalling	1.19	ns	1.21	ns	0.91	ns
NM_000011.9	YAP1	Cell proliferation; Hippo signalling.	0.13	0.001	0.21	0.0016	0.42	0.033
NM_000019.9	AXL	Cell survival	0.54	ns	3.01	0.0021	0.92	ns
NM_000008.10	IKBKB	Cell survival	0.28	0.0043	0.42	0.033	4.78	0.0028
NM_000012.11	NFKB1	Cell survival	0.24	0.001	0.81	ns	3.98	0.023
NM_000002.11	MERTK	Cell survival	6.38	0.0017	1.05	ns	1.69	ns
NM_000020.10	SNAI1	EMT; cell proliferation; cell migration	3.09	0.001	0.98	ns	8.18	0.0008
NM_000009.11	TGFBR1	EMT; cell proliferation; cell migration	0.22	0.0015	0.42	0.028	6.01	0.0023
NM_000007.13	TWIST1	EMT; cell proliferation; cell migration	0.31	0.0013	0.16	0.003	3.81	0.0021
NM_000002.11	TWIST2	EMT; cell proliferation; cell migration	0.97	ns	0.29	0.0026	6.01	0.0039
NM_000010.10	ZEB1	EMT; cell proliferation; cell migration	0.19	0.0014	0.44	0.017	6.11	0.020
NM_000002.11	ZEB2	EMT; cell proliferation; cell migration	0.35	0.0011	0.33	0.0048	9.116	0.0004
NM_000006.11	DDR1	Cell migration	5.92	0.0024	6.21	0.037	5.91	0.046
NM_000008.10	PLAT	Cell migration	6.41	0.0014	1.29	ns	5.71	0.029
NM_000019.9	PLAUR	Cell migration	0.10	0.0032	6.11	0.0011	1.38	ns
NM_000003.11	ALCAM	Cell adhesion; cell migration	0.48	0.043	0.21	0.019	0.11	0.0027
NM_000011.9	CD44	Cell adhesion; cell migration	4.19	0.0016	0.44	0.047	11.09	0.0033
NM_000001.10	CD34	Cell adhesion	0.72	ns	3.09	0.027	0.98	ns
NM_000017.10	FLOT2	Cell adhesion	0.35	0.032	0.93	ns	6.72	0.0003
NM_000005.9	ITGA2	Cell adhesion; cell proliferation	8.03	0.0005	0.19	0.011	16.09	0.0009
NM_000002.11	ITGA4	Cell adhesion; cell proliferation	13.39	0.0014	8.21	0.012	11.14	0.0006
NM_000002.11	ITGA6	Cell adhesion; cell proliferation	3.38	0.0017	2.98	0.038	1.43	ns
NM_000010.10	ITGB1	Cell adhesion; cell proliferation	0.29	0.0039	0.41	0.019	2.56	0.033
NM_000001.10	MUC1	Cell adhesion;	7.38	0.0011	1.98	ns	6.56	0.025

		cell proliferation						
NM_000011.9	THY1	Cell adhesion	0.41	0.0021	4.13	0.0019	4.12	0.0015

Fold-Change (2^(- Delta Delta Ct)) is the normalized gene expression (2^(- Delta Ct)) in IC, divided the normalized gene expression (2^(- Delta Ct)) in AC from the same patient, where Ct is the threshold cycle in qRT-PCR. Fold-change values greater than 1 indicate up-regulation, fold-change values less than 1 indicate down-regulation. The p values are calculated based on a Student's t-test of the replicate 2^(- Delta Ct) values for each gene. $p<0.05$ was considered significant. Epi: epithelioid; sar: sarcomatous; bip: biphasic

Supplementary Table S5. Hematochemical parameters of the treated animals

	Scrambled vehicle	Scrambled Pt+PMX	KO vehicle	KO Pt+PMX
RBC ($x10^6/\mu l$)	11.13±2.34	11.85±2.11	12.18±1.76	11.87±2.76
Hb (g/dl)	13.65±2.65	12.52±2.86	13.78±1.86	12.94±2.94
WBC ($x10^3/\mu l$)	12.02±2.78	12.41±3.08	13.21±2.12	13.44±3.09
PLT ($x10^3/\mu l$)	985±202	1001±189	1197±279	945±208
LDH (U/l)	5432±769	5281±591	5187±813	5412±762
AST (U/l)	169±56	181±52	167±56	194±53
ALT (U/l)	45±13	48±18	50±16	45±16
AP (U/l)	134±31	117±39	146±41	107±33
Creatinine (mg/l)	0.028±0.008	0.031±0.008	0.028±0.008	0.032±0.008
CPK (U/l)	376±83	393±87	381±71	409±94

9-weeks old NOD-SCID-γ Balb/C female mice (n=6/group) were treated as described in **Figure 2i**. Blood was collected immediately after euthanasia and analyzed for red blood cells (RBC), hemoglobin (Hb), white blood cells (WBC), platelets (PLT), lactate dehydrogenase (LDH), aspartate aminotransferase (AST), alanine aminotransferase (ALT), alkaline phosphatase (AP), creatinine, creatine phosphokinase (CPK). Data are means±SD.

Supplementary Table S6. Expression of Wnt-related and target genes in malignant pleural mesothelioma cells

Ref Seq	Gene name	Biological function	Fold change (epi SC vs epi AC)	p value	Fold change (sar SC vs sar AC)	p value	Fold change (bip SC vs bipAC)	p value
NM_000012.11	WNT1	WNT ligand	1.92	0.013	4.22	0.0044	2.89	0.0034
NM_000007.13	WNT2	WNT ligand	1.78	0.016	2.14	0.021	2.09	0.0044
NM_000001.10	WNT2B	WNT ligand	3.70	0.0016	1.79	0.039	4.11	0.0011
NM_000017.10	WNT3	WNT ligand	3.27	0.0013	2.64	0.0012	3.55	0.0026
NM_000001.10	WNT3A	WNT ligand	1.66	0.0043	1.13	ns	1.12	ns
NM_000001.10	WNT4	WNT ligand	1.88	0.0014	2.07	0.0016	1.18	ns
NM_000003.11	WNT5A	WNT ligand	8.93	0.0008	5.45	0.0019	8.11	0.029
NM_000012.11	WNT5B	WNT ligand	3.50	0.0009	3.33	0.012	1.67	0.033
NM_000002.11	WNT6	WNT ligand	1.98	0.0081	4.98	0.0029	2.43	0.0056
NM_000003.11	WNT7A	WNT ligand	6.07	0.0017	4.67	0.0011	4.01	0.002
NM_000022.10	WNT7B	WNT ligand	5.59	0.0013	5.05	0.0018	3.09	0.0016
NM_000005.9	WNT8A	WNT ligand	1.66	0.007	1.18	ns	1.51	0.041
NM_000001.10	WNT9A	WNT ligand	2.67	0.016	1.54	0.0053	1.67	0.048
NM_000002.11	WNT10A	WNT ligand	5.06	0.0015	10.11	0.0019	7.11	0.0023

NM_000011.9	WNT11	WNT ligand	2.27	0.0032	5.11	0.0037	4.17	0.0029
NM_000007.13	WNT16	WNT ligand	11.12	0.0017	8.89	0.0039	8.17	0.0024
NM_000002.11	FRZB	WNT inhibitor	0.37	0.039	2.11	0.039	0.79	ns
NM_000008.10	SFRP1	WNT inhibitor	0.24	0.0023	0.27	0.0017	0.33	0.0033
NM_000004.11	SFRP2	WNT inhibitor	0.35	0.0043	0.39	0.018	0.29	0.013
NM_000007.13	SFRP4	WNT inhibitor	0.73	ns	0.19	0.0007	0.29	0.0019
NM_000012.11	WIF1	WNT inhibitor	0.06	0.001	0.038	0.0015	0.11	0.0015
NM_000007.13	FZD1	WNT receptor	2.23	0.023	1.28	ns	1.87	0.043
NM_000017.10	FZD2	WNT receptor	4.11	0.0019	4.89	0.0019	1.39	ns
NM_000008.10	FZD3	WNT receptor	3.8	0.0005	2.44	0.029	2.56	0.047
NM_000011.9	FZD4	WNT receptor	2.27	0.009	1.19	ns	2.09	0.011
NM_000002.11	FZD5	WNT receptor	3.55	0.0038	1.55	ns	2.18	0.011
NM_000008.10	FZD6	WNT receptor	0.09	0.0011	0.67	ns	0.71	ns
NM_000002.11	FZD7	WNT receptor	1.31	ns	2.38	0.046	2.12	0.024
NM_000010.10	FZD8	WNT receptor	1.78	ns	1.34	ns	1.74	ns
NM_000007.13	FZD9	WNT receptor	1.96	0.014	2.47	0.0012	2.39	0.046
NM_000012.11	LRP1	WNT co-receptor	1.24	ns	1.39	ns	1.29	ns

NM_000011.9	LRP5	WNT co-receptor	0.24	0.0044	1.23	ns	1.13	ns
NM_000012.11	LRP6	WNT co-receptor	0.94	ns	0.83	ns	1.03	ns
NM_000002.11	ANTXR1	WNT signalling activator	8.26	0.0017	2.78	0.019	4.99	0.0029
NM_000001.10	BCL9	WNT signalling activator	6.22	0.0003	2.97	0.0059	4.29	0.0019
NM_000005.9	EGR1	WNT signalling activator	4.69	0.0011	10.19	0.001	3.94	0.0007
NM_000002.11	FN1	WNT activator; WNT target gene	1.39	ns	0.32	0.029	2.12	0.036
NM_000023.10	PORCN	WNT signalling activator	1.07	ns	1.02	ns	1.87	ns
NM_000014.8	DAAM1	WNT signalling activator (non-canonical pathway)	0.19	0.0016	0.38	0.0013	0.21	0.0004
NM_000003.11	RHOA	WNT signalling activator (non-canonical pathway)	1.84	0.024	2.29	0.029	2.17	0.009
NM_000001.10	RHOU	WNT signalling activator (non-canonical pathway)	0.76	ns	0.94	ns	0.42	0.048
NM_000001.10	DVL1	WNT signalling activator (canonical/non-canonical pathway)	5.29	0.0009	6.11	0.0029	4.01	0.0013
NM_000017.10	DVL2	WNT signalling activator (canonical/non-canonical pathway)	4.38	0.0038	1.98	0.0036	4.09	0.0022
NM_000003.11	CTNNB1	WNT signalling activator (canonical pathway)	1.18	ns	0.79	ns	0.89	Ns
NM_000011.9	DIXDC1	WNT signalling activator (canonical pathway)	4.31	0.0013	10.19	0.0018	3.71	0.011
NM_000010.10	FRAT1	WNT signalling activator (canonical pathway)	5.70	0.0011	2.89	0.012	2.58	0.014
NM_000002.11	IRS1	WNT signalling activator (canonical pathway)	10.1	0.0012	3.98	0.017	3.18	0.021
NM_000004.11	LEF1	WNT signalling activator (canonical pathway)	1.72	0.043	2.34	0.0023	2.41	0.0017

NM_000018.9	TCF4	WNT signalling activator (canonical pathway)	3.09	0.0026	3.52	0.0017	4.69	0.0012
NM_000005.9	TCF7	WNT signalling activator (canonical pathway)	2.58	0.0022	4.18	0.0038	2.15	0.0044
NM_000002.11	TCF7L1	WNT signalling activator (canonical pathway)	1.42	ns	1.98	0.041	0.82	ns
NM_000010.10	TCF7L2	WNT signalling activator (canonical pathway)	7.25	0.0012	5.71	0.0032	5.19	0.0007
NM_000001.10	VANGL2	WNT signalling activator (canonical pathway)	0.94	ns	0.22	0.0041	1.18	ns
NM_000004.11	PITX2	WNT signalling actvator (canonical pathway); WNT signalling inhibitor (non-canonical pathway)	1.79	0.016	0.89	ns	1.11	ns
NM_000019.9	AES	WNT signalling inhibitor	0.33	0.013	0.07	0.0003	0.31	0.0009
NM_000007.13	AHR	WNT signalling inhibitor	0.36	ns	0.72	ns	0.71	ns
NM_000019.9	ANGPTL4	WNT signalling inhibitor	0.62	ns	0.72	ns	0.81	ns
NM_000010.10	BTRC	WNT signalling inhibitor	0.69	ns	0.79	ns	0.73	ns
NM_000009.11	TLE1	WNT signalling inhibitor	0.42	0.0014	0.82	ns	0.53	0.049
NM_000005.9	APC	WNT signalling inhibitor (canonical pathway)	0.13	0.0010	0.24	0.0022	0.19	0.0028
NM_000005.9	AXIN1	WNT signalling inhibitor (canonical pathway)	0.25	0.0031	0.19	0.011	0.39	0.0059
NM_000017.10	AXIN2	WNT signalling inhibitor (canonical pathway)	0.28	0.0018	0.11	0.0008	0.01	0.0001
NM_000016.9	CDH1	WNT signalling inhibitor (canonical pathway)	0.17	0.0037	0.44	0.18	0.37	0.0034
NM_000005.9	CSNK1A1	WNT signalling inhibitor (canonical pathway)	0.34	0.027	0.88	ns	0.56	ns
NM_000020.10	CSNK2A1	WNT signalling inhibitor (canonical pathway)	0.24	0.0011	0.31	0.0011	0.51	0.048

NM_000004.11	CTBP1	WNT signalling inhibitor (canonical pathway)	0.04	0.0010	0.28	0.0034	0.29	0.018
NM_000001.10	CTNNBIP1	WNT signalling inhibitor (canonical pathway)	0.37	0.0024	0.26	0.0012	0.25	0.016
NM_000004.11	CXXC4	WNT signalling inhibitor (canonical pathway)	0.66	0.043	0.48	0.0073	0.47	ns
NM_000005.9	DAB2	WNT signalling inhibitor (canonical pathway)	0.26	0.0011	0.27	0.0045	0.72	Ns
NM_000010.10	DKK1	WNT signalling inhibitor (canonical pathway)	0.45	0.014	0.062	0.0027	031	0.037
NM_000011.9	DKK3	WNT signalling inhibitor (canonical pathway)	0.13	0.0013	0.43	0.0039	0.34	0.0041
NM_000005.9	FBXW11	WNT signalling inhibitor (canonical pathway)	0.21	0.0005	0.14	0.0007	0.44	0.047
NM_000010.10	FBXW4	WNT signalling inhibitor (canonical pathway)	0.05	0.0012	0.11	0.0005	0.11	0.0004
NM_000020.10	GDF5	WNT signalling inhibitor (canonical pathway)	3.18	0.0044	4.32	0.047	227	0.0011
NM_000019.9	GSK3A	WNT signalling inhibitor (canonical pathway)	0.98	ns	0.41	0.046	1.01	ns
NM_000003.11	GSK3B	WNT signalling inhibitor (canonical pathway)	1.35	0.199	0.43	0.044	1.16	0.071
NM_000022.10	KREMEN1	WNT signalling inhibitor (canonical pathway)	0.06	0.0013	038	0.0028	0.23	0.0051
NM_000016.9	NKD1	WNT signalling inhibitor (canonical pathway)	0.08	0.0014	0.41	0.038	0.56	ns
NM_000012.11	PRICKLE1	WNT signalling inhibitor (canonical pathway)	0.32	0.015	0.478	ns	0.33	0.047
NM_000009.11	CDKN2A	WNT target gene; inhibitor of cell proliferation	0.35	0.023	047	0.046	0.31	0.038
NM_000010.10	CUBN	WNT target gene	0.30	0.027	0.94	ns	2.87	0.0043
NM_000023.10	EFNB1	WNT target gene	0.15	0.0025	0.43	ns	0.24	0.0032

NM_000007.13	EGFR	WNT target gene	10.1	0.0014	5.66	0.0018	3.48	0.00021
NM_000007.13	NRCAM	WNT target gene	0.07	0.0010	0.89	ns5	10.17	0.0028
NM_000006.11	PPARD	WNT target gene	1.53	ns	1.33	ns	1855	0.018
NM_000001.10	PTGS2	WNT target gene	1.78	0.0024	4.11	0.0027	3.96	0.0016
NM_000008.10	WISP1	WNT target gene	2.6	0.0013	3.07	0.0012	4.26	0.0008
NM_000020.10	WISP2	WNT target gene	13.09	0.0010	4.26	0.0014	5.76	0.0012
NM_000007.13	ABCB1	WNT target gene (canonical pathway)	4.17	0.017	3.52	0.0048	4.24	0.0012
NM_000017.10	BIRC5	WNT target gene (canonical pathway); cell survival	17.03	0.0011	6.78	0.0006	3.83	0.038
NM_000014.8	BMP4	WNT target gene (canonical pathway)	0.75	ns	0.08	0.0007	0.41	0.0049
NM_000011.9	CCND1	WNT target gene (canonical pathway); cell proliferation	7.29	0.016	2.45	0.012	4.37	0.00344
NM_000012.11	CCND2	WNT target gene (canonical pathway); cell proliferation	5.49	0.0014	3.93	0.0017	4.11	0.0006
NM_000008.10	CEBPD	WNT target gene (canonical pathway)	5.49	0.0012	1.89	0.05	1.34	0.052
NM_000006.11	CTGF	WNT target gene (canonical pathway)	1.55	0.037	1.27	0.054	0.86	0.061
NM_000008.10	FGF20	WNT target gene (canonical pathway)	5.43	0.0011	4.38	ns	1.84	0.0047
NM_000011.9	FGF4	WNT target gene (canonical pathway)	10.66	0.0010	6.71	0.0018	4.17	0.0015
NM_000015.9	FGF7	WNT target gene (canonical pathway)	2.1	ns	1.34	ns	2.51	ns
NM_000013.10	FGF9	WNT target gene (canonical pathway)	6.85	0.0005	4.25	0.024	3.26	0.028

NM_000011.9	FOSL1	WNT target gene (canonical pathway)	1.31	ns	2.24	0.041	3.95	0.0014
NM_000017.10	FOXN1	WNT target gene (canonical pathway)	3.66	0.0012	1.43	ns	0.73	ns
NM_000005.9	FST	WNT target gene (canonical pathway)	1.08	ns	0.47	ns	1.28	ns
NM_000006.11	GJA1	WNT target gene (canonical pathway)	8.24	0.0014	7.09	0.0027	4.67	0.0021
NM_000002.11	ID2	WNT target gene (canonical pathway)	0.44	0.048	0.84	ns	1.67	0.043
NM_000012.11	IGF1	WNT target gene (canonical pathway)	9.01	0.0014	4.93	0.0034	3.91	0.0016
NM_000001.10	JUN	WNT target gene (canonical pathway)	3.26	0.024	2.11	0.034	2.46	ns
NM_000007.13	MET	WNT target gene (canonical pathway)	10.08	0.0007	5.44	0.023	2.18	0.029
NM_000016.9	MMP2	WNT target gene (canonical pathway)	3.29	0.0016	3.47	0.039	1.68	0.046
NM_000011.9	MMP7	WNT target gene (canonical pathway)	2.32	0.0022	3.18	0.0076	1.195	ns
NM_000020.10	MMP9	WNT target gene (canonical pathway)	14.24	0.0009	4.56	0.0013	3.76	0.0045
NM_000008.10	MYC	WNT target gene (canonical pathway)	12.18	0.0013	3.98	0.0024	8.14	0.0045
NM_000010.10	NRP1	WNT target gene (canonical pathway)	1.62	0.024	4.01	0.0059	6.13	0.0032
NM_000014.8	SIX1	WNT target gene (canonical pathway)	3.13	0.0012	4.67	0.0048	2.04	0.016
NM_000008.10	SOX17	WNT target gene (canonical pathway)	3.21	0.016	1.56	ns	2.29	0.0056
NM_000007.13	VEGFA	WNT target gene (canonical pathway)	6.91	0.0011	4.43	0.0056	3.12	0.0024
NM_000013.10	KLF5	WNT target gene (canonical/non-canonical pathway)	0.81	ns	0.59	ns	1.01	ns

NM_000010.10	MAPK8	WNT target gene (canonical/non-canonical pathway)	1.14	ns	0.87	ns	1.78	0.045

Fold-Change (2^(- Delta Delta Ct)) is the normalized gene expression (2^(- Delta Ct)) in IC, divided the normalized gene expression (2^(- Delta Ct)) in AC from the same patient, where Ct is the threshold cycle in qRT-PCR. Fold-change values greater than 1 indicate up-regulation, fold-change values less than 1 indicate down-regulation. The p values are calculated based on a Student's t-test of the replicate 2^(- Delta Ct) values for each gene. $p<0.05$ was considered significant. Epi: epithelioid; sar: sarcomatous; bip: biphasic.

Supplementary Table S7. Retrospective analysis of ABCB5 expression and clinical data of patients with diagnosed malignant pleural mesothelioma

UPN	Age (years)	Histotype	Intensity of ABCB5 staining	First-line treatment	TTP (months)	OS (months)
1	59	Epi	+	Pt+PMX	unknown	116
2	48	Epi	+	Pt+PMX	7	11
3	71	Epi	+	cPt+PMX	14	24
4	71	Epi	+	cPt+PMX	8	11
5	68	Epi	+	Pt+PMX	9	15
6	78	Epi	++	PMX	unknown	24
7	61	Epi	+	Pt+PMX	7	15
8	72	Epi	++	Pt+PMX	unknown	52
9	74	Bip	++	cPt+PMX	6	19
10	64	Epi	++	Pt+PMX	11	23
11	60	Sar	++	Pt+PMX	unknown	4
12	74	Epi	++	cPt+PMX	unknown	2
13	55	Sar	+++	cPt+PMX	3	7
14	62	Epi	+	Pt+PMX	23	30
15	73	Epi	+	Pt+PMX	16	19
16	69	Epi	++	Pt+PMX	5	8
17	66	Epi	+	Pt+PMX +/- nintedanib	9	11
18	66	Epi	++	cPt+PMX	8	10
19	71	Epi	+	cPt+PMX	7	14
20	74	Epi	+++	Pt+PMX +/- nintedanib	unknown	7
21	75	Epi	++	PMX	3	5
22	76	Epi	++	cPt+PMX	4	5
23	75	Epi	+	Pt+PMX +/- nintedanib	12	31
24	71	Epi	+	Pt+PMX +/- nintedanib	28	30
25	73	Epi	++	Pt+PMX +/- nintedanib	11	12
26	70	Epi	+	Pt+PMX	unknown	6
27	67	Epi	+++	cPt+PMX	9	15
28	71	Epi	++	cPt+PMX	11	17
29	76	Epi	++	cPt+PMX	4	13
30	66	Epi	+++	cPt+PMX	11	15
31	71	Epi	++	cPt+PMX	5	6
32	70	Epi	++	cPt+PMX	8	13
33	64	Epi	+++	Pt+PMX	6	20
34	46	Epi	+	Pt+PMX	16	21
35	62	Epi	+	Pt+PMX	11	14
36	74	Epi	+	cPt+PMX	unknown	15
37	69	Epi	++	Pt+PMX	5	7

Age, MPM histotype, mean intensity of ABCB5 by immunohistochemical staining, treatment and clinical data, for the patient analyzed retrospectively. UPN: unknown patient number. Age: age at diagnosis. Epi: epithelioid; Sar; sarcomatous; Bip: biphasic. Pt: cisplatin; cPt: carboplatin; PMX: pemetrexed. TTP: time to progression: time from the start of treatment to the first sign of disease's progression. OS: overall survival: survival from the beginning of therapy until patients exitus.